



**Bromine partitioning
in the TTL**

R. P. Fernandez et al.

This discussion paper is/has been under review for the journal Atmospheric Chemistry and Physics (ACP). Please refer to the corresponding final paper in ACP if available.

Bromine partitioning in the tropical tropopause layer: implications for stratospheric injection

R. P. Fernandez¹, R. J. Salawitch², D. E. Kinnison³, J.-F. Lamarque³, and A. Saiz-Lopez¹

¹Atmospheric Chemistry and Climate Group, Institute of Physical Chemistry Rocasolano, CSIC, Madrid 28006, Spain

²Department of Atmospheric and Oceanic Science, Department of Chemistry and Biochemistry, and Earth System Science Interdisciplinary Center, University of Maryland, College Park, Maryland, MD 20742, USA

³Atmospheric Chemistry Division, NCAR, Boulder, CO 80301, USA

Received: 29 May 2014 – Accepted: 20 June 2014 – Published: 3 July 2014

Correspondence to: A. Saiz-Lopez (a.saiz@csic.es)

Published by Copernicus Publications on behalf of the European Geosciences Union.

Title Page

Abstract

Introduction

Conclusions

References

Tables

Figures



Back

Close

Full Screen / Esc

Printer-friendly Version

Interactive Discussion



Abstract

Very short-lived (VSL) bromocarbons are produced at a prodigious rate by ocean biology and these source compounds (SG_{VSL}), together with their degradation inorganic products (PG_{VSL}), are lofted by vigorous convection to the tropical tropopause layer (TTL). Using a state-of-the-art photochemical mechanism within a global model, we calculate annual average stratospheric injection of total bromine due to VSL sources to be 5 pptv, with ~ 3 pptv entering the stratosphere as PG_{VSL} and ~ 2 pptv as SG_{VSL} . The geographic distribution and partitioning of VSL bromine within the TTL, and its consequent stratospheric injection, is highly dependent on the oceanic flux, the strength of convection and the occurrence of heterogeneous recycling reactions. Our calculations indicate atomic Br should be the dominant inorganic species in large regions of the TTL during daytime, due to the low ozone and cold conditions of this region. We propose the existence of a “tropical ring of atomic bromine” located approximately between 15 and 19 km and 30° N to 30° S. Daytime Br / BrO ratios of up to ~ 4 are predicted within the Br ring in regions of highly convective transport, such as the tropical Western Pacific. Then, we suggest experimental programs designed to quantify the bromine budget of the TTL and the stratospheric injection of VSL biogenic bromocarbons should include a strategy for the measurement of atomic Br during daytime and HOBr or BrCl during nighttime.

1 Introduction

Bromine compounds produced by biogenic processes in the oceans may influence the composition of the global atmosphere via their decomposition and the subsequent influence of the resulting bromine radicals on the tropospheric and stratospheric ozone budget, oxidation of elemental mercury and dimethyl sulphide (DMS) (Saiz-Lopez and von Glasow, 2012). Contributions of these biogenic sources, commonly known as very-short lived (VSL) bromocarbons, to inorganic bromine (Br_y) in the stratosphere (Salaw-

ACPD

14, 17857–17905, 2014

Bromine partitioning in the TTL

R. P. Fernandez et al.

Title Page

Abstract

Introduction

Conclusions

References

Tables

Figures



Back

Close

Full Screen / Esc

Printer-friendly Version

Interactive Discussion



itch et al., 2005; Salawitch, 2006) would have important climatic effects on ozone photochemistry and trends (Dorf et al., 2006; Sinnhuber et al., 2009), and have been proposed as the missing contribution required to reconcile measurements and model simulations of stratospheric bromine chemistry (Montzka et al., 2011).

5 Considerable effort is presently being extended towards quantifying the oceanic production (Carpenter and Liss, 2000; Quack and Wallace, 2003; Pyle et al., 2011; Leedham et al., 2013; Liu et al., 2013) and convective transport (Ashfold et al., 2012; Fuhlbrügge et al., 2013) of biogenic VSL bromocarbons, as well as understanding the chemical transformations of these compounds to inorganic bromine species in
10 the atmosphere ((Yang et al., 2005; Hossaini et al., 2010; Salawitch, 2006; Parrella et al., 2012; Saiz-Lopez et al., 2012; Sommariva and von Glasow, 2012; Aschmann and Sinnhuber, 2013)). Several global halocarbon emission inventories have been developed (Warwick et al., 2006; Liang et al., 2010; Ordóñez et al., 2012; Ziska et al.,
15 2013) and compared (Hossaini et al., 2013) to address the contribution of VSL bromocarbons to the photochemistry of the troposphere and the stratospheric bromine injection. The short photochemical lifetime of many biogenic VSL bromocarbons (i.e. weeks to months, see Table 1) results in photochemical breakdown and release of reactive bromine atoms in the troposphere (Montzka et al., 2011), mainly in the tropical tropopause layer (TTL). The quantification of brominated organic source gas (SG) and
20 inorganic product gas (PG) distributions in the TTL is of great importance for determining the impact of the VSL bromocarbons on the ozone budget of the free troposphere and lowermost stratosphere (Salawitch et al., 2005; Montzka et al., 2011; Aschmann and Sinnhuber, 2013).

25 While many global model simulations indicate that the SG injection or carbon-bonded portion (SG_{VSL}) is the dominant contribution of VSL bromocarbons to stratospheric bromine loading (Aschmann et al., 2009; Hossaini et al., 2010, 2012; Aschmann and Sinnhuber, 2013), the combination of heterogeneous recycling processes and rapid gaseous cycling of the inorganic PG species (PG_{VSL} , also referred hereafter as Br_y) increases the lifetime of the more hydrophilic inorganic portion (Parrella et al., 2012;

**Bromine partitioning
in the TTL**

R. P. Fernandez et al.

Title Page

Abstract

Introduction

Conclusions

References

Tables

Figures



Back

Close

Full Screen / Esc

Printer-friendly Version

Interactive Discussion



**Bromine partitioning
in the TTL**

R. P. Fernandez et al.

Title Page

Abstract

Introduction

Conclusions

References

Tables

Figures



Back

Close

Full Screen / Esc

Printer-friendly Version

Interactive Discussion



Aschmann and Sinnhuber, 2013). Hence, the amount of inorganic bromine injected to the stratosphere is critically dependent on the balance between the efficiency of Br_y removal by aerosol-, water- and ice-uptake (followed by particle sedimentation) and the occurrence of heterogeneous reactions that recycle photolabile PG_{VSL} species back to the gaseous phase (Sinnhuber and Folkins, 2006; Liang et al., 2010; Aschmann et al., 2011; Ordóñez et al., 2012; Aschmann and Sinnhuber, 2013). Additionally, the local convection would directly affect the timescale of the vertical transport (Aschmann et al., 2009; Hossaini et al., 2010; Ashfold et al., 2012), which also influences the SG_{VSL} and PG_{VSL} lifetimes.

Experimental campaigns are underway to measure the abundance and speciation of a host of organic bromine species and the dominant inorganic compounds within the TTL (Dorf et al., 2008; Brinckmann et al., 2012; ATTREX, 2014; CAST, 2014; CONTRAST, 2014; Wisher et al., 2014), because this region is critical for quantifying the fate of biogenic bromine decomposition products and their impact on atmospheric chemistry (Hossaini et al., 2012; Saiz-Lopez et al., 2012; Aschmann and Sinnhuber, 2013). Here we highlight some of the unique aspects of the TTL that drive the partitioning of inorganic bromine species by means of combined global- and box-modeling simulations. Based on our results, we discuss implications for the understanding of inorganic bromine chemistry and transport within the TTL, and assess its relevance on estimations of stratospheric bromine injection from VSL bromocarbon sources.

1.1 The tropical tropopause layer

The tropopause transition layer or tropical tropopause layer is the region between the lapse rate minimum at ~ 12 km (i.e., with a zero radiative heating potential temperature $\theta_{ZRH} \approx 350$ K) and the cold point tropopause ($\theta_{CPT} \approx 380$ K, at ~ 17 km; see Gettelman and Forster, 2002). Most gases that enter the stratosphere are first transported upwards by deep convection that detrains within the TTL (Sinnhuber and Folkins, 2006), followed by large-scale ascent.

2.1 CAM-Chem setup

The setup used here considers a horizontal grid resolution of 1.9° (latitude) \times 2.5° (longitude) and 26 hybrid vertical levels from the surface to approximately 40 km (Ordóñez et al., 2012; Saiz-Lopez et al., 2012). The model can be configured to perform either climatic simulations in “free running” mode (FR), where the physical state of the atmosphere is allowed to evolve independently following the hydrostatic equations; or in “specified dynamics” mode (SD), where high frequency offline meteorological fields are used to compute the dynamical transport. The SD procedure can allow for more precise comparisons between measurements of atmospheric composition and model output, and also allow to compare different sensitivity simulations where the chemical perturbations can be distinguished from the transport changes related to the physical state of the atmosphere (Lamarque et al., 2012).

To avoid dynamical perturbations, present simulations were performed in SD mode considering a high frequency meteorological input from a previous CAM-Chem 15 year long climatic simulation. In this way, our CAM-Chem setup implies that we force the system to evolve as if it was a CTM (Chemical Transport Model), resolving the complexity of the novel tropospheric/stratospheric halogen-chemistry mechanism while using the meteorological fields from a standard chemistry-climate simulation. Then, the horizontal wind components, air temperature, surface temperature, surface pressure, sensible and latent heat flux and wind stress are read from the input meteorological dataset every 3–6 h, while for time-steps between the reading times, all fields are linearly interpolated to avoid jumps. Even when in this work CAM-Chem is used as a CTM, the model is allowed to proceed with an independent inter-annual chemical evolution of all tropospheric and stratospheric constituents, and a direct comparison of the oxidative capacity of different types of atmospheres (e.g. with tropospheric bromine chemistry and without it) can be addressed (see Lamarque et al. (2012) for a complete description of this specific type of configuration). The model is configured with prescribed sea

Bromine partitioning in the TTL

R. P. Fernandez et al.

[Title Page](#)[Abstract](#)[Introduction](#)[Conclusions](#)[References](#)[Tables](#)[Figures](#)[Back](#)[Close](#)[Full Screen / Esc](#)[Printer-friendly Version](#)[Interactive Discussion](#)

surface temperatures (SST) and ice-coverage for the 2000 decade (Rayner, 2003), so results are not representative of the meteorology of any specific year.

2.1.1 Bromine chemistry scheme

The model version used here includes a state-of-the-art organic and inorganic halogen (i.e. chlorine and bromine) photochemistry mechanism, considering both natural and anthropogenic sources, heterogeneous recycling, dry and wet deposition, both in the troposphere and stratosphere (see Supplement in Ordóñez et al., 2012). Rate constants have been updated to JPL-2010 (Sander et al., 2011) and IUPAC-2008 (Atkinson et al., 2007, 2008). The chemical solver in all simulations is initialized with identical chemical boundary conditions for any given species, and all the atmospheric oxidants are computed online at all times (i.e., without considering prescribed monthly OH fields as done in previous studies). As major improvements with respect to previous studies are related to heterogeneous recycling over ice-particles and wet deposition processes; in Sects. 2.1.3 and 2.1.4 we present details of the implementation of these methods in CAM-Chem.

2.1.2 VSL bromocarbon emissions inventory

Geographically and seasonally distributed natural oceanic sources of VSL bromo- and iodo-carbons have been included and validated in the model (Ordóñez et al., 2012). The top-down emissions inventory includes monthly varying oceanic fluxes based on parameterizations of chlorophyll *a* satellite maps within the tropical oceans (20° N–20° S) with a 2.5 coast-to-ocean emission ratio. In the extra tropics (20–50° and 50–90°) a seasonal latitudinal variation is also considered. The current setup includes bromocarbon sources of CHBr₃, CH₂Br₂, CH₂BrCl, CHBr₂Cl and CHBrCl₂, while iodocarbon species include CH₃I, CH₂I₂, CH₂ICl and CH₂I₂Br. Hereafter SG_{VSL} = CHBr₃, CH₂Br₂, CH₂BrCl, CHBr₂Cl, CHBrCl₂ and CH₂I₂Br. The anthropogenic halogen lower boundary conditions are based on prescribed surface concentrations of long-lived species

Bromine partitioning in the TTL

R. P. Fernandez et al.

Title Page

Abstract

Introduction

Conclusions

References

Tables

Figures



Back

Close

Full Screen / Esc

Printer-friendly Version

Interactive Discussion



(CFCs, CH₃Cl, CH₃Br and Halons H1301, H1211, H1202, H2402) representative of year 2000. The long-lived inventory is based on Meinshausen et al. (2011), and has been recently used in IPCC AR5 hindcast and projection simulations (Marsh et al., 2013).

The global Br mass flux from all VSL bromocarbons is approximately 630 Gg Br yr⁻¹, comparable to our previous model estimates (Ordóñez et al., 2012). Table 1 presents the individual emission contribution from each VSL considered, as well as their respective photochemical lifetime and the annual tropical surface mixing ratios that the inclusion of the emissions inventory generates. The geographical and seasonal representation of VSL sources constitutes a major improvement in CAM-Chem relative to studies performed with other models, where constant surface mixing ratios of VSL halocarbons are imposed at the lower level (Hossaini et al., 2012; Aschmann and Sinnhuber, 2013). Indeed, the current CAM-Chem setup includes constant surface mixing ratios only for long-lived species, because their long lifetimes ensure tropospheric homogenization.

2.1.3 Heterogeneous recycling

Mechanistic improvements with respect to previous works (Ordóñez et al., 2012; Saiz-Lopez et al., 2012) are mainly based on the implementation of tropospheric heterogeneous reactions for HBr, HOBr and BrONO₂ on ice particles and aerosol surfaces. The inclusion of these reactions in CAM-Chem is based on the stratospheric implementation of heterogeneous recycling processes of Kinnison et al. (2007). Table S1 in the supplement presents the full set of chlorine and bromine heterogeneous reactions occurring on different types of surfaces (i.e., stratospheric sulfate aerosols (SULF), nitric acid tri-hydrate (NAT), ice particles (ICE) and sea-salt (SSLT) aerosols) with their respective reactive uptake coefficients (γ). For the case of liquid sulfate aerosols, a physically-based treatment of heterogeneous kinetics (γ_{SULF}) following the framework of Hanson et al. (1994) is applied. All heterogeneous reactions occurring over ice surfaces with the exception of the ones for HBr were considered in our previous model configurations, although a different latitudinal/vertical efficiency below the tropopause was

Bromine partitioning in the TTL

R. P. Fernandez et al.

Title Page

Abstract

Introduction

Conclusions

References

Tables

Figures



Back

Close

Full Screen / Esc

Printer-friendly Version

Interactive Discussion



applied. Reactive uptake coefficients from Crowley et al. (2010), Ammann et al. (2013) and JPL-2010 (Sander et al., 2011) were used, unless stated otherwise.

Heterogeneous recycling reactions of HOBr, BrNO₂ and BrONO₂ (and their equivalent chlorine compounds) are also considered to proceed on sea-salt aerosol surfaces (SA_{SSLT}), considering that the rate limiting step is the uptake of halogen species on the aerosol surface (McFiggans et al., 2000). Note that this process represents an additional source of inorganic bromine and chlorine in the troposphere, independent from the oceanic flux of VSL halocarbons described above (i.e. these are non-stoichiometric reactions releasing Cl and Br atoms from sea-salt aerosols to the gas phase). The contribution of SSLT heterogeneous reactions to the Br_y loading for different geographical regions is analyzed in Sect. 3.4.

2.1.4 Washout and ice-uptake

The removal of halogen species in CAM-Chem occurs via washout and scavenging in water and ice clouds (Lamarque et al., 2012; Ordóñez et al., 2012), treating each of the Br_y species independently. The Henry Law's coefficients (k_H) for all bromine and chlorine species included in the model are shown in Table S2. Values are taken from the compilation of Henry's Law constants of Sander (1999).

As nighttime reservoir species are more likely to be adsorbed by water/ice particles and removed from the gaseous phase (Crowley et al., 2010; Ammann et al., 2013), the modeled Br_y loading in the TTL depends on the efficiency of the wet deposition schemes (such as in-cloud washout or removal by ice-uptake) relative to the heterogeneous recycling (Aschmann et al., 2011; Aschmann and Sinnhuber, 2013). CAM-Chem has been updated to include ice-uptake removal of halogen species following an equivalent procedure to that used by Neu and Prather (2012) for HNO₃. Several sensitivity studies showed that an extremely efficient and unrealistic washout of Br_y was artificially introduced in the case of considering ice-uptake for HBr, HOBr and other bromine acids. Then, the novel NEU scheme in CAM-Chem (Lamarque et al., 2012) was implemented with ice-uptake turned on for all chlorine species and for BrONO₂,

Bromine partitioning in the TTL

R. P. Fernandez et al.

Title Page

Abstract

Introduction

Conclusions

References

Tables

Figures



Back

Close

Full Screen / Esc

Printer-friendly Version

Interactive Discussion



BrNO₂, BrCl and Br₂, considering that the removal of this reservoir halogen species occurs at liquid, ice, and mixed-phase clouds in the troposphere (Neu and Prather, 2012). For the rest of Br_y species (BrO, HOBr, HBr) the NEU scheme was implemented only for liquid clouds (washout).

Several studies have determined that the efficiency of HBr recycling on ice particles greatly surpass the net uptake into the condensed phase, and ice-mediated HBr losses within the TTL were estimated to represent at most 2% of the actual loss rate when a full chemistry scheme is considered (Aschmann et al., 2011). Then, even when inorganic bromine removal in the lower troposphere is highly dependent on k_H (HBr), its impact decreases within the TTL. Indeed, due to the very fast photochemical time constants for the Br_y system that rapidly equilibrate the steady-state abundance of all bromine species, bromine scavenging from the gaseous phase can proceed via the washout of other species besides HBr. For example, the ice-uptake for BrONO₂, one of the most abundant nighttime reservoirs in the absence of heterogeneous recycling, is considered to be infinitely efficient (i.e. it is instantaneously removed from the gaseous phase once it collides with an ice-particle, see Sander and Crutzen, 1996; Sander, 1999) and controls the bromine burden in the upper TTL.

2.2 Box-model configuration

We have used a photochemical box-model (Salawitch et al., 2005) to compute the concentration of inorganic bromine species throughout a daily cycle, subject to the constraint that production and loss of each species is balanced over a 24 h period (diurnal photochemical steady state). The model includes a representation of 36 species constrained by specified values of p , T , O₃, Br_y, Cl_y, NO_y, H₂O, CH₄, CO, as well as particle surface area. Reaction rates and absorption cross-sections are from JPL-2010 (Sander et al., 2011). With the exception of the ozone sensitivity study (Sect. 3.3.1), all box-model simulations had been performed with an ambient O₃ concentration of 25 ppbv, which is the expected ozone value existent in the TTL. The abundance of H₂O is set at 12.5 ppm, the saturation mixing ratio for $T = 200$ K and $p = 130$ hPa. Values of

Bromine partitioning in the TTL

R. P. Fernandez et al.

Title Page

Abstract

Introduction

Conclusions

References

Tables

Figures



Back

Close

Full Screen / Esc

Printer-friendly Version

Interactive Discussion



**Bromine partitioning
in the TTL**

R. P. Fernandez et al.

Title Page

Abstract

Introduction

Conclusions

References

Tables

Figures



Back

Close

Full Screen / Esc

Printer-friendly Version

Interactive Discussion



NO_y are based on observations (Murphy et al., 1993). The abundance of CO is based on recent measurements in the subtropical upper troposphere (Marcy et al., 2004) and the value of CH_4 is set to contemporary surface levels. Surface Area for sulfate (SA_{SULF}) had been estimated from SAGE II measurements, obtained during July 2005.

5 SA_{ICE} was found assuming a condensation of 12.5 ppmv of H_2O onto 10 particles cm^{-3} , resulting in 7.5 μm radius particles. Clearly, SA_{ICE} in the TTL is highly variable. Our calculations are designed to represent the fact that typically, $\text{SA}_{\text{ICE}} \gg \text{SA}_{\text{SULF}}$ in the TTL (see Fig. 10). Reactive uptake coefficients for the heterogeneous recycling reactions were taken from JPL-2010 (Sander et al., 2011), based on the laboratory measurements of Abbatt (1994). Unless stated otherwise, all simulations were performed
10 for $\text{Lat} = 10^\circ \text{N}$ and $\text{Solar Decl} = 20^\circ$, and numerical values for all model inputs are as follow: $p = 130 \text{ hPa}$, $T = 200 \text{ K}$, $\text{H}_2\text{O} = 12.5 \text{ ppmv}$, $\text{CH}_4 = 1.77 \text{ ppmv}$, $\text{CO} = 60 \text{ ppbv}$, $\text{Br}_y = 4 \text{ pptv}$, $\text{NO}_y = 400 \text{ pptv}$ and $\text{O}_3 = 25 \text{ ppbv}$. Model output for the box-model simulations is shown as $[X]/[\text{Br}_y]$, where $[X]$ represents the mixing ratio of specific inorganic
15 bromine species. We have conducted simulations for $\text{Br}_y = 4 \text{ pptv}$, but all results shown here are extremely insensitive to the particular choice of Br_y , for values ranging from at least 1 to 10 pptv. Results are also insensitive to input values of H_2O and CO.

3 Results and discussions

All the CAM-Chem results shown here include an ocean mask below 3 km altitude
20 to avoid considering grids above land that could produce artificially reduced vertical profiles within the marine boundary layer (MBL). Besides the standard 24 h averaged streaming, time dependent output for day and night has been generated considering the noon (11:30–12:30) and midnight (23:30–00:30) LT, respectively, for all latitudes and longitudes. Tropical averages have been computed between 20°N – 20°S , while the Western Pacific (WP) warm pool area is defined by the equator (0°) and the 20°N
25 parallels, and the 120°E and 165°E meridians (see black rectangle in Fig. 5).

3.1 The partitioning of inorganic and organic bromine

The vertical distribution of annually averaged inorganic bromine species within the tropics (20° N–20° S) at noon and midnight is shown in Fig. 1a and b, respectively. Figure 1c illustrates the 24 h-mean inorganic and organic contributions to the total bromine budget of the tropical atmosphere. Our model shows a total ($\text{Br}_{\text{total}} = \text{Br}_{\text{org}} + \text{Br}_{\text{y}}$) stratospheric bromine loading of ~ 21 pptv, within the range of values (19.5–24.5 pptv) inferred from measurements of stratospheric BrO reported in the last WMO ozone assessment report (Montzka et al., 2011). Below the tropopause, Br_{org} (defined as $\text{Br}_{\text{Halons}} + \text{CH}_3\text{Br} + \text{SG}_{\text{VSL}}$) is the dominant form of bromine because the abundant long-lived bromocarbons have not yet decomposed. Within this organic portion, ~ 4.3 pptv of SG_{VSL} reaches the lower TTL, where 2.3 pptv are transformed to active Br_{y} before stratospheric injection (see Fig. 2 and Table 1 for details on the individual SG_{VSL} partitioning). In the middle and upper stratosphere (i.e., above ~ 25 km altitude), inorganic bromine dominates because of photodissociation of any organic compounds that cross the tropopause (Fig. 1c).

HBr is the dominant inorganic bromine species in the MBL, free troposphere (FT) and lower TTL both during daytime and at night (Fig. 1a and b). Then, the removal rate of HBr controls the total amount of Br_{y} that reaches the lower TTL and can subsequently be injected into the stratosphere (Yang et al., 2005; Sinnhuber and Folkins, 2006; Parrella et al., 2012; Aschmann and Sinnhuber, 2013). In the upper TTL, $\text{HBr}/\text{Br}_{\text{y}} \sim 0.1$ due to fast heterogeneous recycling over ice-particles that releases reactive bromine back to the gas phase, so bromine washout is controlled by the scavenging of nighttime reservoirs. On an annual average, noontime BrO values in the FT are ~ 0.2 pptv within the tropics (Fig. 1a) and in the range 0.2–0.4 pptv for mid-latitudes (Fig. 6), with higher values of up to a few pptv calculated for certain coastal locations within the MBL, in agreement with previous studies (Yang et al., 2005; Parrella et al., 2012; Saiz-Lopez et al., 2012). The modeled tropical vertical profiles of BrO are in excellent agreement with balloon measurements performed in the tropical regions where BrO concentrations of

Bromine partitioning in the TTL

R. P. Fernandez et al.

Title Page

Abstract

Introduction

Conclusions

References

Tables

Figures

◀

▶

◀

▶

Back

Close

Full Screen / Esc

Printer-friendly Version

Interactive Discussion



(2.0 ± 1.5) pptv for the local tropopause (17 km) and (3.2 ± 1.6) pptv at 18 km were observed, with very low, or even negligible, BrO concentrations (< 1 ppt) for the lower, middle and upper troposphere (Dorf et al., 2008).

During nighttime, BrONO₂ and HOBr dominate the inorganic bromine budget in the TTL and stratosphere, while HBr dominates in the FT and MBL (Fig. 1b). The abundance of BrCl in the upper TTL increases due to the efficient heterogeneous recycling of inorganic chlorine reservoirs (Cl_y). The potential importance of BrCl is quite uncertain due to two factors: (i) the contribution of VSL chlorocarbons to Cl_y in the upper TTL is not well constrained by observations but likely is between 0 and 50 pptv (Montzka et al., 2011); (ii) the particle habitat is highly variable and the ClO/Cl_y ratio is quite sensitive to temperature. A box-model sensitivity analysis of the recycling processes affecting the partitioning of nighttime bromine reservoirs is given in Sect. 3.3.

The tropical annual vertical profiles for all VSL bromocarbons and their overall SG_{VSL} contribution are shown in Fig. 2a. The equivalent profiles computed for February within the WP region are presented in Fig. 2b. The Br_y loading within the TTL depends primarily on the release of reactive bromine from CHBr₃ and CH₂Br₂, which are the most abundant species and represent more than 85 % of SG_{VSL} in the lower TTL (Montzka et al., 2011). CHBr₃ is removed mainly by photolysis (it has the smallest lifetime of VSL bromocarbons), releasing an annual average of 1.7 pptv Br atoms into the gaseous inorganic phase before being transported to the stratosphere (see Table 1). In comparison, only ~ 17 % of the bromine contained in CH₂Br₂ that reaches the lower TTL is released below the cold point tropopause (~ 17 km). Within the WP region, where the strength of convective transport is increased, 5.1 pptv of SG_{VSL} reach the lower TTL. Also, due to the faster vertical transport, the photochemical loss of CHBr₃ within the TTL is reduced by ~ 35 %, releasing only ~ 1.1 pptv Br before stratospheric injection occurs. Comparatively, only 5 % of CH₂Br₂ is decomposed before stratospheric injection.

**Bromine partitioning
in the TTL**

R. P. Fernandez et al.

Title Page

Abstract

Introduction

Conclusions

References

Tables

Figures

⏪

⏩

◀

▶

Back

Close

Full Screen / Esc

Printer-friendly Version

Interactive Discussion



3.2 The tropical ring of atomic bromine

Daytime levels of atomic Br increase significantly within the TTL due to the low abundance of ozone and cold conditions, which restrict formation of BrO by the Br + O₃ reaction. As a result we simulate a daytime “tropical ring of atomic bromine” extending from 30° N to 30° S (Fig. 3), where Br atoms constitute a major portion of Br_y. Within this tropical ring, annual average Br maximizes at ~ 1.3 pptv near the cold point tropopause, representing up to 30 % of the total annually-averaged Br_y within the tropics (see contour lines in Fig. 3).

The tropical ring of atomic Br is a photochemical phenomenon. It exists only on the illuminated portion of the earth, so it circles the tropics with the sun. The tropical ring extends approximately from 15 to 19 km, driven by vertical variations in ozone and temperature. The height thickness is delimited by temperatures colder than ~ 200 K, with O₃ mixing ratios ranging between 50 ppbv and 500 ppbv at the bottom and top boundaries, respectively. Below the lower limit of the ring, the ambient temperature is high enough (e.g. > 220 K) for the highly exothermic Br + O₃ reaction (Sander et al., 2011) to proceed efficiently. Above the ring, in the lower stratosphere, ozone abundances of a few ppmv and warmer conditions lead to the rapid formation of BrO through Br + O₃.

The existence of the atomic Br ring is a direct consequence of the O₃/*T* dependences described above, and as such, presents a marked seasonality and geographical distribution (see Figs. 3c and 5a). The maximum abundances of atomic Br within the tropical ring are coincident with low ozone regions, i.e., in geographical areas of extremely strong convection such as the tropical WP warm pool (Ashfold et al., 2012; Brinckmann et al., 2012), where O₃-poor air masses originating from the MBL are rapidly transported to the lower TTL (Folkins and Braun, 2002). Our results indicate atomic Br levels up to 3 pptv may occur in the WP region during periods of vigorous convection (Fig. 4). Due to the fast vertical transport during convective events (hours to days), SG_{VSL} have not yet decomposed, and the source of Br_y in the lower TTL is indeed the efficient sea-salt recycling occurring in the MBL. Model sensitivities (Sect. 3.4)

Bromine partitioning in the TTL

R. P. Fernandez et al.

[Title Page](#)[Abstract](#)[Introduction](#)[Conclusions](#)[References](#)[Tables](#)[Figures](#)[Back](#)[Close](#)[Full Screen / Esc](#)[Printer-friendly Version](#)[Interactive Discussion](#)

indicate that during strong convection, approximately half of the Br_y entrained from the MBL into the fast uplifting transport reaches the lower TTL ($\text{Br}_y^{\text{MBL}} \approx 7$ pptv and $\text{Br}_y^{12\text{km}} \approx 3.5$ pptv).

3.2.1 The Br/BrO ratio in the TTL

Even though BrO is the most abundant species throughout the tropics on an annual average (Fig. 1a), a ratio of $\text{Br}/\text{BrO} > 1$ will occur in key areas. The abundance of atomic Br surpasses BrO in regions of the TTL where temperatures and O_3 levels range from 190 K to 220 K and from 50 ppbv to 25 ppbv, respectively (see Figs. 4 and 5). As Br and BrO establish a photochemical steady-state, their ratio can be approximated by the BrO photolysis (J_{BrO}) and the exothermic $\text{Br} + \text{O}_3$ reaction ($k_{\text{Br}+\text{O}_3}$), i.e., $[\text{Br}]/[\text{BrO}] = J_{\text{BrO}}/(k_{\text{Br}+\text{O}_3}[\text{O}_3])$. A box-modeling analysis of the sensitivity of the partitioning between Br and BrO to ozone is given in Sect. 3.3.1.

The Br/BrO ratio peaks in regions with $\text{O}_3 < 40$ ppbv and $T < 190$ K, while for regions with $\text{O}_3 > 60$ ppbv and $T > 200$ K within the tropics a ratio of $\text{Br}/\text{BrO} < 1$ is found. The altitude where the Br/BrO ratio peaks is usually located just below the maximum level of atomic Br, as a consequence of a compromise between the decrease of temperature and the increase of O_3 towards the lower stratosphere.

The magnitude of the Br/BrO ratio peak strongly depends on season and geographical region, due to the changes in oceanic sources and vertical transport. Figure 5a–c shows the modeled geographic distributions of Br, BrO and Br/BrO ratio at the top of the TTL (~ 17 km) for February. At this altitude, monthly averaged values of $\text{Br}/\text{BrO} \sim 2.5$ are found for the WP region. The WP is a critical region: during Northern Hemisphere winter, a majority of air parcels that are lofted to the $\theta_{\text{CPT}} = 380$ K level by rapid convection (which marks likely future ascent to the stratosphere) detrain in the TTL (Bergman et al., 2012). For individual events of vigorous convection within the WP, atomic Br represents $\sim 60\%$ of daytime Br_y and a maximum Br/BrO ratio of ~ 4 is found (see Fig. 4b).

Bromine partitioning in the TTL

R. P. Fernandez et al.

[Title Page](#)[Abstract](#)[Introduction](#)[Conclusions](#)[References](#)[Tables](#)[Figures](#)[⏪](#)[⏩](#)[◀](#)[▶](#)[Back](#)[Close](#)[Full Screen / Esc](#)[Printer-friendly Version](#)[Interactive Discussion](#)

**Bromine partitioning
in the TTL**

R. P. Fernandez et al.

Title Page

Abstract

Introduction

Conclusions

References

Tables

Figures



Back

Close

Full Screen / Esc

Printer-friendly Version

Interactive Discussion



Figure 6 shows the zonal average vertical distribution of BrO abundances between 60° N–60° S, similar to Fig. 3a for atomic Br. The characteristic latitudinal variation of the tropopause is clearly defined by the change in BrO abundances: within the tropics, the altitude of the tropopause is ~ 17 km or ~ 100 hPa while for the mid-latitudes remains between 10–12 km (~ 200 hPa). Within the FT, BrO abundances remain below 0.4 pptv on an annual average, while in the stratosphere up to 70 % of Br_y is due to BrO, with a clear stratification as we move up to the higher levels. At the top of the model (~ 35 km), daytime BrO reaches 16 pptv, and together with BrONO₂ and HOBr are the most abundant species in the sunlit stratosphere.

Even when the geographic distributions of Br and BrO differ (Fig. 5a and b), the Br/BrO ratio follows the spatial patterns of O₃ and temperature (Fig. 5d and e). This confirms that the Br/BrO ratio is nearly independent of the total amount of Br_y (Fig. 5f), as expected due to the rapid photochemical time constants of the Br_y system (Salawitch et al., 2005; Saiz-Lopez and von Glasow, 2012). Notwithstanding uncertainties in heterogeneous reactions and removal processes, all the global sensitivity simulations presented in Sect. 3.4 predict the existence of the tropical ring of atomic bromine and a pronounced Br/BrO peak within the TTL. Hence, measurements of the abundance of daytime Br, in addition to that of BrO, would be valuable for quantifying the bromine budget in the TTL and the injection of Br_y to the stratosphere.

3.3 Sensitivity to heterogeneous recycling: a box-modelling approach

The species HBr, HOBr and BrONO₂ are soluble and likely to be absorbed by aerosol or liquid cloud particles (Iraci et al., 2005; Abbatt et al., 2012; Saiz-Lopez and von Glasow, 2012), and the reactive uptake of HBr and HOBr has been observed to proceed over ice (Abbatt, 1994). Depending on the local microphysical environment, sedimentation of these particles and dehydration could represent an efficient sink for Br_y, preventing the decomposition products of biogenic bromocarbons from reaching the lower stratosphere (Sinnhuber and Folkins, 2006) or global troposphere (Yang et al., 2005). However, the efficiency of aerosol/cloud washout of Br_y is likely altered by heteroge-

neous reactions that release bromine to the gas phase (Iraci et al., 2005; Salawitch, 2006; Sinnhuber and Folkins, 2006), and several recent global modeling studies have included HBr heterogeneous recycling with different efficiencies and highlighted its importance (Yang et al., 2005; Aschmann et al., 2011; Parrella et al., 2012; Aschmann and Sinnhuber, 2013). Here we go a step forward and, instead addressing the bromine removal efficiency, we focus on the important changes in the nighttime partitioning of bromine reservoirs due to the inclusion (or not) of heterogeneous recycling reactions. Table 2 presents a complete set of kinetic model sensitivities aimed at evaluating the uncertainties of such processes for atmospheric conditions representative of the cold point tropopause of the tropical WP. Results are shown for various model runs, with different assumptions for particle surface area (SA) and total inorganic chlorine (Cl_y) affecting the heterogeneous reactions



Once inorganic bromine is produced from the decomposition of biogenic bromine compounds, we expect the chemistry to equilibrate rapidly to a state similar to one of those shown in Fig. 7. In all cases, the nighttime reservoirs are converted almost entirely to Br and BrO during each sunlit cycle, with HBr being the only other species potentially present during daytime. The particular state will be determined by local ambient levels of O_3 , temperature, Cl_y , as well as particle surface area.

Figure 7b shows the diurnal variation of Br_y species for *Run_1a*, which assumes the presence of only sulfate aerosols (SA_{SULF}) and that $Cl_y = 0$. The calculated abundance of $BrONO_2$ displays a rapid rise during evening twilight, because the nighttime buildup of NO_2 occurs coincident with the presence of BrO. However, $BrONO_2$ is converted to HOBr by heterogeneous hydrolysis, with a lifetime of several hours (Lary et al., 1996). Prior to sunrise, the Br_2 produced by Reaction (R1) constitutes about 20 % of Br_y , being HOBr the dominant nighttime reservoir. If the recycling reaction is turned off (*Run_0*, where $\gamma_{HOBr+HBr} = 0$), significant levels of HBr are present at all times (Fig. 7a) and

**Bromine partitioning
in the TTL**

R. P. Fernandez et al.

Title Page

Abstract

Introduction

Conclusions

References

Tables

Figures

◀

▶

◀

▶

Back

Close

Full Screen / Esc

Printer-friendly Version

Interactive Discussion



**Bromine partitioning
in the TTL**

R. P. Fernandez et al.

Title Page

Abstract

Introduction

Conclusions

References

Tables

Figures



Back

Close

Full Screen / Esc

Printer-friendly Version

Interactive Discussion



the lowest values of atomic Br are found. On the other hand, in the presence of large areas of ice particles (SA_{ICE}), the heterogeneous Reaction (R1) acts as a rapid sink of HBr, resulting in nearly complete nighttime conversion of all Br_y to HOBr (Fig. 7c). Reaction (R1) has been observed to proceed on ice (Abbatt, 1994) and sulfate surfaces (Iraci et al., 2005) under laboratory settings, so it is likely that the conditions of *Run_0* are unrealistic. Hence, very low abundances of HBr are expected to be present in the TTL. Figure 7d shows calculated lifetimes for photochemical loss of HBr; the longest time constant is for *Run_0*, with HBr removal becoming progressively faster for *Run_1a* and *Run_1b*.

The nighttime partitioning of Br_y species is also sensitive to the possible presence of trace chlorine. Background chlorine levels in the FT and lower TTL are < 10 pptv due to the long photolytic lifetimes of CFCs and CH_3Cl , and the small contributions from VSL chlorocarbons (Montzka et al., 2011). Despite this, stratospheric intrusion events are frequent within the TTL, and observations of Cl_y as high as 50 pptv have been reported in the subtropical upper troposphere (Marcy et al., 2004). The presence of this much Cl_y results in rapid conversion of HOBr to BrCl, due to Reaction (R2). As shown in Fig. 7e and f, BrCl will likely be the dominant nighttime Br_y reservoir whenever $Cl_y \gg Br_y$ (for *Run_2a*, Br_2 is the other nighttime reservoir). Abundances of Cl_y large enough to drive nighttime Br_y almost entirely into BrCl might be supplied either by decomposition of VSL chlorocarbons, or by irreversible mixing of a small portion of stratospheric air into the upper troposphere (Marcy et al., 2004).

3.3.1 Dependence of Br_y partitioning on ozone and temperature

Figure 8 shows the box-model calculated noontime abundance of Br_y species, as a function of O_3 for *Run_0*. The vertical dashed lines denote O_3 mixing ratios of 20 and 30 ppbv, values commonly present near convective outflow in the TTL. For these levels of O_3 , atomic Br is the dominant inorganic species during daytime, representing at least 50 % of the total inorganic Br_y . For values of $O_3 = 25$ ppbv, the Br/ Br_y and HBr/ Br_y ratios display a slight sensitivity to total NO_y (400 pptv), but Br and BrO remain

**Bromine partitioning
in the TTL**

R. P. Fernandez et al.

Title Page

Abstract

Introduction

Conclusions

References

Tables

Figures



Back

Close

Full Screen / Esc

Printer-friendly Version

Interactive Discussion



the dominant daytime species for all values of NO_y reported by Murphy et al. (1993) for the TTL. In regions with higher ozone abundances (i.e. > 100 ppbv), as in the lower stratosphere, the diurnal Br–BrO steady-state is displaced to favor the BrO production.

The sensitivity of noontime Br/Br_y , BrO/Br_y , and HBr/Br_y to temperature is shown in Fig. 9. For these calculations, $\text{O}_3 = 25$ ppbv and H_2O is set to its temperature dependent saturation mixing ratio, although nearly identical results are found if H_2O is kept constant at 12.5 ppmv. The simulations show that for temperatures less than ~ 200 K, atomic Br is expected to constitute at least half of total Br_y . Model results shown by the solid lines are for *Run_1a* conditions. The temperature sensitivity is driven by the $\text{Br} + \text{O}_3$, $\text{Br} + \text{H}_2\text{CO}$, $\text{Br} + \text{HO}_2$, and $\text{BrO} + \text{NO}$ rate constants, each of which acts to increase the Br/Br_y ratio and decrease the HBr/Br_y ratio, with decreasing temperature. The uncertainty in the calculated abundances of Br, BrO, and HBr due to gas phase and heterogeneous processes is shown by the dashed and dotted lines in Fig. 9a–c. For gas phase processes, the uncertainty of individual kinetic parameters is based on JPL-2010 (Sander et al., 2011). The uncertainty due to heterogeneous processes considers cases *Run_0* and *Run_2b* (see Supplement).

3.4 Global model sensitivities to processes and sources

Table 3 describes a set of 5 global sensitivity simulations that were performed with CAM-Chem to quantify the contribution of each source gas to the PG_{VSL} and SG_{VSL} bromine burden. Besides including the surface oceanic flux of only a unique VSL source gas or turning ON/OFF the heterogeneous reactions, the rest of the parameterizations considered in the chemical scheme are identical to those used for the baseline simulation (*cam_Full_Br*). To avoid extraneous chemical perturbations related to differences in stratospheric halogen loading of bromine and chlorine, all simulations considered identical boundary conditions for long-lived halocarbon species (i.e., CFCs, CH_3Br and halons).

Table 4 presents values of PG_{VSL} and SG_{VSL} as well as the total bromine loading due to VSL sources (ΣBr) for the lower TTL (12 km) and upper TTL (17 km), for various re-

gions and averaging periods. Note that for the *cam_NoVSL* simulation, SG_{VSL} includes the contribution of all long-lived bromocarbons, while the PG_{VSL} portion represents the Br_y decomposition products released by photolysis of CH_3Br below the tropopause. Table 4 also presents the R quotient for each CAM-Chem sensitivity simulation, computed as:

$$R = \frac{PG_{VSL}}{SG_{VSL}}. \quad (1)$$

As CAM-Chem includes a complete treatment of halogen chemistry within the troposphere, the term PG_{VSL} in the numerator is the sum of: (i) the decomposition products from the SG_{VSL} entering the lower TTL, (ii) and the vertical transport of Br_y reaching the lower TTL from the FT and MBL. For the *cam_CHBr3*, *cam_CH2Br2* and *cam_MinorVSL* runs PG_{cam_NoVSL} is subtracted from the numerator to account for stratospheric injection of product gases resulting from tropospheric degradation of CH_3Br . Several global modeling studies oriented to determine the magnitude of the stratospheric bromine injection due to VSL do not consider a detailed treatment of the tropospheric halogen chemistry, and then approximate the entrainment of Br_y from the lower troposphere.

CAM-Chem sensitivities indicate that on an annual average, the Br_y abundance in the upper TTL can be up to one order of magnitude greater than SG_{VSL} if only $CHBr_3$ sources are considered ($R \sim 10$). In comparison, when only CH_2Br_2 is taken into account, $R < 0.3$ due to the greater photochemical lifetime of this source (see Table 4) and only 0.3 pptv of bromine is released from the SG_{VSL} to the inorganic portion below the tropopause. During convective events, the photo-degradation of bromocarbons within the TTL account only for a small portion of the Br_y loading: between 12 and 17 km, the SG_{VSL} reduction is ~ 0.06 , 0.1 and 1.0 pptv for *cam_MinorVSL*, *cam_CH2Br2* and *cam_CHBr3*, respectively. This highlights the importance of considering the different dynamical timescales of large-scale ascent and deep convective events, as well as a detailed tropospheric chemical mechanism, when computing the partitioning between SG_{VSL} and PG_{VSL} of short-lived species.

**Bromine partitioning
in the TTL**

R. P. Fernandez et al.

Title Page

Abstract

Introduction

Conclusions

References

Tables

Figures

◀

▶

◀

▶

Back

Close

Full Screen / Esc

Printer-friendly Version

Interactive Discussion



**Bromine partitioning
in the TTL**

R. P. Fernandez et al.

Title Page

Abstract

Introduction

Conclusions

References

Tables

Figures

◀

▶

◀

▶

Back

Close

Full Screen / Esc

Printer-friendly Version

Interactive Discussion



The entrainment of Br_y into the TTL from the lower troposphere constitutes an important portion (~ 1.0 pptv when all VSL sources are considered for the tropical annual average) of the PG_{VSL} component to stratospheric injection (see Table 4). Photodegradation of CHBr_3 represents $\sim 90\%$ of the annual PG_{VSL} reaching the lower TTL even when heterogeneous recycling on sea-salt aerosol is not considered. Indeed, integrated in the tropics SSLT recycling can account, at most, for about 10% of the Br_y levels at 12 km, and only 3% of the total PG_{VSL} at 17 km. The situation changes considerably during events of vigorous convection within the WP region. There, the Br_y loading at the lower TTL is significantly reduced from 3.6 pptv for *cam_Full_Br* to 0.5 pptv for *cam_noSSLT*. Then, in strong convective regions the Br_y loading is dominated by the entrainment of product gases from the FT and MBL instead of being controlled by VSL degradation (see below).

3.4.1 Implications of heterogeneous recycling reactions on the composition of the TTL

Figure 10 shows vertical profiles for the main variables affecting the heterogeneous rates for Reactions (R1) ($\text{HBr} + \text{HOBr}$) and (R2) ($\text{HCl} + \text{HOBr}$) considering the baseline *cam_Full_Br* simulation. The vertical variation of the surface area density of ice particles (SA_{ICE}), liquid droplets (SA_{LIQ}) and sulfate aerosols (SA_{SULF}) between 20°N – 20°S is presented in Fig. 10a. Within the TTL, SA_{ICE} densities are at least one order of magnitude greater than those for SA_{SULF} , therefore ice-mediated heterogeneous reactions are expected to predominate within the TTL in agreement with other modeling studies (Aschmann and Sinnhuber, 2013). The SA_{ICE} density for the tropical annual average (solid lines) can be up to a factor of 10 smaller than for the WP region during February (dashed lines). This indicates that in regions of strong convection the efficiency of heterogeneous reactions within the TTL can be considerably enhanced. Indeed, the rapid uplift of air-masses and the colder temperatures increase the total amount of ice-cloud droplets where heterogeneous reactions occur (Williams et al., 2009)

**Bromine partitioning
in the TTL**

R. P. Fernandez et al.

Title Page

Abstract

Introduction

Conclusions

References

Tables

Figures



Back

Close

Full Screen / Esc

Printer-friendly Version

Interactive Discussion



Our box-model sensitivities indicate that the other important factor controlling the efficiency of heterogeneous recycling of HBr and HOBr is the total amount of inorganic chlorine available as HCl. Figure 10b shows the vertical profile abundance of HCl and Cl_y for the tropical annual average and the WP region during February. Levels up to 50 pptv on an annual average are modeled within the tropics in agreement with previous reports (Marcy et al., 2004), although WP abundances remain below 10 pptv within the TTL, due to the faster vertical transport of VSL-chlorocarbons that decreases the release of chlorine atoms.

In the absence of solar radiation, BrCl is the dominant bromine nocturnal reservoir at 17 km within the WP region (see Fig. 11), indicating that the current implementation of heterogeneous recycling in CAM-Chem is more sensitive to the increase in SA_{ICE} than to the decrease in Cl_y levels within the high convective regions. Note in Fig. 10c that the efficiency of Reactions (R1) and (R2) within the TTL is at least one order of magnitude greater for the reactions occurring over SA_{ICE} than over SA_{SULF} , being the latter the dominant substrate for recycling only above 20 km. Note that there still are very large uncertainties on both the vertical and geographical representation of SA_{ICE} fields in chemical climate models (Williams et al., 2009; Aschmann and Sinnhuber, 2013) and the reactive uptake efficiencies of heterogeneous processes for halogen species (Crowley et al., 2010; Ammann et al., 2013). Hence, field measurements of BrCl, HOBr and other bromine nighttime reservoirs, as well as laboratory measurements of SA_{ICE} reactions would shed some light in the understanding of these fundamental processes.

3.4.2 Impact of convective transport on the bromine burden and partitioning

Figure 11 shows the distribution of the day-/night-time inorganic and organic vertical profile partitioning within the tropical WP during February, in a manner equivalent to Fig. 1, which showed equivalent model results for an annual average of the entire tropics. Several aspects of the sources and processes controlling the bromine partitioning are evident comparing Figs. 1 and 11. First, there is a clear predominance of atomic Br as the most abundant Br_y species during daytime, which corresponds to a stronger

**Bromine partitioning
in the TTL**

R. P. Fernandez et al.

Title Page

Abstract

Introduction

Conclusions

References

Tables

Figures

◀

▶

◀

▶

Back

Close

Full Screen / Esc

Printer-friendly Version

Interactive Discussion



formation of the tropical ring of atomic bromine, as well as a marked increase in the Br/BrO ratio in the WP (see Fig. 4). Second, BrCl becomes the most abundant bromine species during midnight, in agreement with the box-model sensitivity studies performed for the *Run_2a* and *Run_2b* cases. The role of heterogeneous recycling in the TTL highlights the importance of reducing the uncertainties related to the efficiency and temperature dependence of these reactions, and their competition relative to complete washout or ice-removal from the atmosphere (Sinnhuber and Folkins, 2006; Aschmann and Sinnhuber, 2013). Third, both the organic and inorganic bromine burden of the TTL is enhanced within this region. Then, within the WP region during strong convection periods, the ratio Br/BrO > 1 throughout the TTL, and atomic Br represents up to 60 % of total Br_y.

3.5 Implications for stratospheric injection and atmospheric ozone

Our simulations suggest that the proportion of inorganic Br input to the stratosphere is higher ($PG_{VSL} \approx 3$ pptv) than the contribution from the carbon-bonded portion ($SG_{VSL} \approx 2$ pptv), resulting in a total stratospheric bromine injection of ~ 5 pptv. Tropospheric degradation of the long-lived bromine species CH₃Br makes an important contribution, 0.6 pptv, to the total amount of inorganic bromine ($PG_{VSL} \approx 3$ pptv) that is transported across the tropopause (see Table 4). CH₃Br is not commonly considered to be a VSL compound because its atmospheric removal lifetime of ~ 9.6 months is slightly longer than the 6 month cut off used to denote very short lived species (Montzka et al., 2011). However, we consider stratospheric injection of Br_y compounds produced following the tropospheric decomposition of CH₃Br to be part of PG_{VSL} because the ozone destruction potential of bromine in the lowermost stratosphere (LMS) depends critically on the amount of active bromine above the tropopause, regardless of origin (Salawitch et al., 2005). This highlights the need for climate models to incorporate a complete treatment of tropospheric bromine chemistry that includes both VSL and long-lived bromocarbons.

**Bromine partitioning
in the TTL**

R. P. Fernandez et al.

Title Page

Abstract

Introduction

Conclusions

References

Tables

Figures



Back

Close

Full Screen / Esc

Printer-friendly Version

Interactive Discussion



Our global simulations reveal distinctive features in the partitioning of SG_{VSL} and PG_{VSL} between air masses injected to the stratosphere within the WP region and the average tropics (see Figs. 1 and 11, and Table 4). First, VSL bromocarbons are produced at a remarkable rate by ocean biology within the WP, primarily in shallow coastal waters, and are subsequently transported by strong convection to the TTL. As expected, the faster the air masses are transported, the smaller the photolytic release of atomic bromine from VSL bromocarbons and the stronger the injection of the organic SG_{VSL} fraction (Figs. 2b and 11c). Second, the rapid transport of Br_y -rich air masses from the MBL to the lower TTL reduces the wet-deposition of PG_{VSL} species, additionally increasing the Br_y abundance in the WP TTL. This result in a local enhancement of the total bromine loading at θ_{CPT} of 7.7 pptv for the WP region during February (with both SG_{VSL} and PG_{VSL} coincidentally reaching 3.85 pptv) compared to the annual average injection of 5 pptv. Third, during the fast uplifting event that results in the Br/BrO peak shown in Fig. 4, the SG_{VSL} (4.6 pptv) $>$ PG_{VSL} (3.0 pptv) suggests that the tropical ring of atomic bromine exists even when $R < 1$. Finally, note that in the case of the tropical annual average the Br_y loading in the TTL is controlled by SG_{VSL} decomposition (mostly $CHBr_3$, Fig. 2a) and the sea-salt contribution represents $< 3\%$ of the PG_{VSL} reaching the upper TTL.

4 Summary and conclusions

Our estimate of the stratospheric injection of bromine compounds, naturally emitted from the oceans, suggests that the inorganic bromine injected to the stratosphere is larger (~ 3 pptv) than that from very short-lived bromocarbons (~ 2 pptv). Then, accounting for the contributions from all VSL bromocarbons, an overall quotient $R = PG_{VSL}/SG_{VSL} \sim 1.5$ (dominated by the $CHBr_3$ partitioning) is obtained. This result differs from previous model studies that reported that the SG_{VSL} injection is the dominant contribution (Hossaini et al., 2012; Aschmann and Sinnhuber, 2013), or that SG_{VSL} and Br_y contributions are equivalent (Liang et al., 2010), although those reports

considered either constant surface mixing ratios of VSL bromocarbons or a simplified representation of inorganic bromine chemistry and removal processes.

The current CAM-Chem scheme includes geographically and seasonally varying VSL emissions as well as a detailed representation of the multi-phase photochemistry from the ocean surface to the upper stratosphere. Then, our model captures regions where surface halocarbon fluxes are relatively large (i.e., coastal areas) and represents the rapid, deep convective updraft of these air masses to the lower TTL (i.e. WP region). The independent representation of removal processes for each species (HOB_r, HBr, BrONO₂, etc.) allows improved consideration of the various deposition processes (i.e., scavenging in-cloud precipitation, below-cloud washout, large-scale removal and re-evaporation, etc.) that affect the upper atmosphere inorganic bromine loading. In addition, the consideration of sea-salt recycling reactions within the MBL and its convective transport, allow us to account for an additional geographically varying natural source of Br_y to the lower TTL.

As shown above, a substantial portion of the bromine supplied by VSL bromocarbons is available in active form before reaching the LMS. Low ozone and temperature conditions make bromine atoms the dominant inorganic species during the sunlit tropical upper troposphere, generating a natural ring of atomic bromine that circles the tropics with the sun. If confirmed by observation, the tropical ring of atomic bromine would be indicative of direct supply of inorganic bromine to the LMS by biogenic VSL bromocarbons. The inorganic bromine injection to the LMS has the most important effect on stratospheric ozone during times of high sulfate aerosol loading after major volcanic eruptions (Salawitch et al., 2005), following the convection injection of water vapor (Anderson et al., 2012), or under proposed scenarios to artificially increase the stratospheric aerosol burden to mitigate climate change (Tilmes et al., 2012). Then, the supply of inorganic bromine from VSL would likely render the ozone layer more sensitive to future changes in ocean biogeochemistry than current predictions, since most chemistry-climate models presently neglect oceanic bromocarbons sources or detailed tropospheric bromine chemistry.

Bromine partitioning in the TTL

R. P. Fernandez et al.

Title Page

Abstract

Introduction

Conclusions

References

Tables

Figures



Back

Close

Full Screen / Esc

Printer-friendly Version

Interactive Discussion



**Bromine partitioning
in the TTL**

R. P. Fernandez et al.

Title Page

Abstract

Introduction

Conclusions

References

Tables

Figures



Back

Close

Full Screen / Esc

Printer-friendly Version

Interactive Discussion



Heterogeneous reactions of HBr and HOBr are key uncertainties in quantifying the fate of inorganic products produced following the decomposition of biogenic bromocarbons. The fingerprint of heterogeneous reactions is revealed by the behavior of nighttime reservoirs and the abundance of daytime HBr and atomic Br. Therefore, speciated measurements of atomic bromine during the day and nighttime BrCl and/or HOBr in the TTL would provide insight into the nature of heterogeneous chemical processes, which are profoundly important because they potentially regulate the efficiency of Br_y removal by particle sedimentation.

Our modeled contribution of VSL bromocarbons and their breakdown products to stratospheric Br_y represents an increment of ~ 25 % to the stratospheric bromine burden supplied by long-lived sources (CH₃Br and halons). This percentage will likely rise in the future as the atmospheric burden of long-lived sources declines due to a near cessation of anthropogenic emission. If the production and transport of VSL bromocarbons is found to be sensitive to climatically driven changes in the state of the world's oceans (atmospheric winds, sea surface temperature, upwelling, and/or nutrient supply), then the tropical Br ring represents a potentially important new link between climate change and atmospheric ozone. All of this highlights the importance of including a detailed description of the interaction between surface fluxes, convective transport and halogen photochemistry in chemistry-climate model simulations.

**The Supplement related to this article is available online at
doi:10.5194/acpd-14-17857-2014-supplement.**

Acknowledgements. This work was supported by the Consejo Superior de Investigaciones Científicas (CSIC), Spain. The National Center for Atmospheric Research (NCAR) is funded by the National Science Foundation NSF. Computing resources (ark:/85065/d7wd3xhc) were provided by the Climate Simulation Laboratory at NCAR's Computational and Information Systems Laboratory (CISL), sponsored by the NSF. The CESM project (which includes CAM-Chem) is supported by the NSF and the Office of Science (BER) of the US Department of Energy.

This work was also sponsored by the NASA Atmospheric Composition Modeling and Analysis Program Activities (ACMAP), grant/cooperative agreement number NNX11AH90G and NNX12AB10G as well as the NASA Modeling and Analysis Program grant NNX12ZDA001N. We gratefully appreciate the collaboration with Paul Wennberg at an early stage of this research, who suggested BrO would titrate to Br under the low O₃ conditions of the tropical troposphere. R.P.F. would like to thank CONICET and UTN/UNCuyo for prorogating the designation as Assistant Researcher in Argentina in order to continue the postdoc position at CSIC, Spain.

References

- Abbatt, J. P. D.: Heterogeneous reaction of HOBr with HBr and HCl on ice surfaces at 228 K, *Geophys. Res. Lett.*, 21, 665–668, doi:10.1029/94GL00775, 1994.
- Abbatt, J. P. D., Thomas, J. L., Abrahamsson, K., Boxe, C., Granfors, A., Jones, A. E., King, M. D., Saiz-Lopez, A., Shepson, P. B., Sodeau, J., Toohey, D. W., Toubin, C., von Glasow, R., Wren, S. N., and Yang, X.: Halogen activation via interactions with environmental ice and snow in the polar lower troposphere and other regions, *Atmos. Chem. Phys.*, 12, 6237–6271, doi:10.5194/acp-12-6237-2012, 2012.
- Ammann, M., Cox, R. A., Crowley, J. N., Jenkin, M. E., Mellouki, A., Rossi, M. J., Troe, J., and Wallington, T. J.: Evaluated kinetic and photochemical data for atmospheric chemistry: Volume VI – heterogeneous reactions with liquid substrates, *Atmos. Chem. Phys.*, 13, 8045–8228, doi:10.5194/acp-13-8045-2013, 2013.
- Anderson, J. G., Wilmouth, D. M., Smith, J. B., and Sayres, D. S.: UV dosage levels in summer: increased risk of ozone loss from convectively injected water vapor, *Science*, 337, 835–839, doi:10.1126/science.1222978, 2012.
- Aschmann, J. and Sinnhuber, B.-M.: Contribution of very short-lived substances to stratospheric bromine loading: uncertainties and constraints, *Atmos. Chem. Phys.*, 13, 1203–1219, doi:10.5194/acp-13-1203-2013, 2013.
- Aschmann, J., Sinnhuber, B.-M., Atlas, E. L., and Schaufli, S. M.: Modeling the transport of very short-lived substances into the tropical upper troposphere and lower stratosphere, *Atmos. Chem. Phys.*, 9, 9237–9247, doi:10.5194/acp-9-9237-2009, 2009.

**Bromine partitioning
in the TTL**

R. P. Fernandez et al.

Title Page

Abstract

Introduction

Conclusions

References

Tables

Figures

I ◀

▶ I

◀

▶

Back

Close

Full Screen / Esc

Printer-friendly Version

Interactive Discussion



- Aschmann, J., Sinnhuber, B.-M., Chipperfield, M. P., and Hossaini, R.: Impact of deep convection and dehydration on bromine loading in the upper troposphere and lower stratosphere, *Atmos. Chem. Phys.*, 11, 2671–2687, doi:10.5194/acp-11-2671-2011, 2011.
- Ashfold, M. J., Harris, N. R. P., Atlas, E. L., Manning, A. J., and Pyle, J. A.: Transport of short-lived species into the Tropical Tropopause Layer, *Atmos. Chem. Phys.*, 12, 6309–6322, doi:10.5194/acp-12-6309-2012, 2012.
- Atkinson, R., Baulch, D. L., Cox, R. A., Crowley, J. N., Hampson, R. F., Hynes, R. G., Jenkin, M. E., Rossi, M. J., and Troe, J.: Evaluated kinetic and photochemical data for atmospheric chemistry: Volume III – gas phase reactions of inorganic halogens, *Atmos. Chem. Phys.*, 7, 981–1191, doi:10.5194/acp-7-981-2007, 2007.
- Atkinson, R., Baulch, D. L., Cox, R. A., Crowley, J. N., Hampson, R. F., Hynes, R. G., Jenkin, M. E., Rossi, M. J., Troe, J., and Wallington, T. J.: Evaluated kinetic and photochemical data for atmospheric chemistry: Volume IV – gas phase reactions of organic halogen species, *Atmos. Chem. Phys.*, 8, 4141–4496, doi:10.5194/acp-8-4141-2008, 2008.
- ATTREX: Airborne Tropical Tropopause Experiment Project, Funded by NASA, available at: <https://espo.nasa.gov/missions/attrex> (last access: 18 December 2013), 2014.
- Bergman, J. W., Jensen, E. J., Pfister, L., and Yang, Q.: Seasonal differences of vertical-transport efficiency in the tropical tropopause layer: on the interplay between tropical deep convection, large-scale vertical ascent, and horizontal circulations, *J. Geophys. Res.*, 117, D05302, doi:10.1029/2011JD016992, 2012.
- Brinckmann, S., Engel, A., Bönisch, H., Quack, B., and Atlas, E.: Short-lived brominated hydrocarbons – observations in the source regions and the tropical tropopause layer, *Atmos. Chem. Phys.*, 12, 1213–1228, doi:10.5194/acp-12-1213-2012, 2012.
- Carpenter, L. J. and Liss, P. S.: On temperate sources of bromoform and other reactive organic bromine gases, *J. Geophys. Res.*, 105, 20539–20547, doi:10.1029/2000JD900242, 2000.
- CAST: Coordinated Airborne Studies in the Tropics Project, Facil. Airborne Atmos. Meas., available at: <http://www.faam.ac.uk/index.php/current-future-campaigns/384-cast-2014-co-ordinated-airborne-studies-in-the-tropics> (last access: 18 December 2013), 2014.
- CONTRAST: CONvective TRansport of Active Species in the Tropics Project/Earth Observing Laboratory, Funded by NCAR UCAR NSF, available at: https://www.eol.ucar.edu/field_projects/contrast (last access: 18 December 2013), 2014.

**Bromine partitioning
in the TTL**

R. P. Fernandez et al.

Title Page

Abstract

Introduction

Conclusions

References

Tables

Figures



Back

Close

Full Screen / Esc

Printer-friendly Version

Interactive Discussion



Crowley, J. N., Ammann, M., Cox, R. A., Hynes, R. G., Jenkin, M. E., Mellouki, A., Rossi, M. J., Troe, J., and Wallington, T. J.: Evaluated kinetic and photochemical data for atmospheric chemistry: Volume V – heterogeneous reactions on solid substrates, *Atmos. Chem. Phys.*, 10, 9059–9223, doi:10.5194/acp-10-9059-2010, 2010.

5 Dorf, M., Butler, J. H., Butz, A., Camy-Peyret, C., Chipperfield, M. P., Kritten, L., Montzka, S. A., Simmes, B., Weidner, F., and Pfeilsticker, K.: Long-term observations of stratospheric bromine reveal slow down in growth, *Geophys. Res. Lett.*, 33, L24803, doi:10.1029/2006GL027714, 2006.

10 Dorf, M., Butz, A., Camy-Peyret, C., Chipperfield, M. P., Kritten, L., and Pfeilsticker, K.: Bromine in the tropical troposphere and stratosphere as derived from balloon-borne BrO observations, *Atmos. Chem. Phys.*, 8, 7265–7271, doi:10.5194/acp-8-7265-2008, 2008.

15 Emmons, L. K., Walters, S., Hess, P. G., Lamarque, J.-F., Pfister, G. G., Fillmore, D., Granier, C., Guenther, A., Kinnison, D., Laepple, T., Orlando, J., Tie, X., Tyndall, G., Wiedinmyer, C., Baughcum, S. L., and Kloster, S.: Description and evaluation of the Model for Ozone and Related chemical Tracers, version 4 (MOZART-4), *Geosci. Model Dev.*, 3, 43–67, doi:10.5194/gmd-3-43-2010, 2010.

Folkens, I. and Braun, C.: Tropical ozone as an indicator of deep convection, *J. Geophys. Res.*, 107, 4184, doi:10.1029/2001JD001178, 2002.

20 Fuhlbrügge, S., Krüger, K., Quack, B., Atlas, E., Hepach, H., and Ziska, F.: Impact of the marine atmospheric boundary layer conditions on VLSL abundances in the eastern tropical and subtropical North Atlantic Ocean, *Atmos. Chem. Phys.*, 13, 6345–6357, doi:10.5194/acp-13-6345-2013, 2013.

Gettelman, A. and Forster, P. M. D. F.: A climatology of the tropical tropopause layer, *J. Meteorol. Soc. Jpn.*, 80, 911–924, doi:10.2151/jmsj.80.911, 2002.

25 Hanson, D. R., Ravishankara, A. R., and Solomon, S.: Heterogeneous reactions in sulfuric acid aerosols: a framework for model calculations, *J. Geophys. Res.*, 99, 3615, doi:10.1029/93JD02932, 1994.

Hossaini, R., Chipperfield, M. P., Monge-Sanz, B. M., Richards, N. A. D., Atlas, E., and Blake, D. R.: Bromoform and dibromomethane in the tropics: a 3-D model study of chemistry and transport, *Atmos. Chem. Phys.*, 10, 719–735, doi:10.5194/acp-10-719-2010, 2010.

30 Hossaini, R., Chipperfield, M. P., Feng, W., Breider, T. J., Atlas, E., Montzka, S. A., Miller, B. R., Moore, F., and Elkins, J.: The contribution of natural and anthropogenic very short-lived

**Bromine partitioning
in the TTL**

R. P. Fernandez et al.

Title Page

Abstract

Introduction

Conclusions

References

Tables

Figures



Back

Close

Full Screen / Esc

Printer-friendly Version

Interactive Discussion



species to stratospheric bromine, *Atmos. Chem. Phys.*, 12, 371–380, doi:10.5194/acp-12-371-2012, 2012.

Hossaini, R., Mantle, H., Chipperfield, M. P., Montzka, S. A., Hamer, P., Ziska, F., Quack, B., Krüger, K., Tegtmeier, S., Atlas, E., Sala, S., Engel, A., Bönisch, H., Keber, T., Oram, D., Mills, G., Ordóñez, C., Saiz-Lopez, A., Warwick, N., Liang, Q., Feng, W., Moore, F., Miller, B. R., Marécal, V., Richards, N. A. D., Dorf, M., and Pfeilsticker, K.: Evaluating global emission inventories of biogenic bromocarbons, *Atmos. Chem. Phys.*, 13, 11819–11838, doi:10.5194/acp-13-11819-2013, 2013.

Iraci, L. T., Michelsen, R. R., Ashbourn, S. F. M., Rammer, T. A., and Golden, D. M.: Uptake of hypobromous acid (HOBr) by aqueous sulfuric acid solutions: low-temperature solubility and reaction, *Atmos. Chem. Phys.*, 5, 1577–1587, doi:10.5194/acp-5-1577-2005, 2005.

Kinnison, D. E., Brasseur, G. P., Walters, S., Garcia, R. R., Marsh, D. R., Sassi, F., Harvey, V. L., Randall, C. E., Emmons, L., Lamarque, J. F., Hess, P., Orlando, J. J., Tie, X. X., Randel, W., Pan, L. L., Gettelman, A., Granier, C., Diehl, T., Niemeier, U., and Simmons, A. J.: Sensitivity of chemical tracers to meteorological parameters in the MOZART-3 chemical transport model, *J. Geophys. Res.*, 112, D20302, doi:10.1029/2006JD007879, 2007.

Lamarque, J.-F., Emmons, L. K., Hess, P. G., Kinnison, D. E., Tilmes, S., Vitt, F., Heald, C. L., Holland, E. A., Lauritzen, P. H., Neu, J., Orlando, J. J., Rasch, P. J., and Tyndall, G. K.: CAM-chem: description and evaluation of interactive atmospheric chemistry in the Community Earth System Model, *Geosci. Model Dev.*, 5, 369–411, doi:10.5194/gmd-5-369-2012, 2012.

Lary, D. J., Chipperfield, M. P., Toumi, R., and Lenton, T.: Heterogeneous atmospheric bromine chemistry, *J. Geophys. Res.*, 101, 1489–1504, doi:10.1029/95JD02839, 1996.

Leedham, E. C., Hughes, C., Keng, F. S. L., Phang, S.-M., Malin, G., and Sturges, W. T.: Emission of atmospherically significant halocarbons by naturally occurring and farmed tropical macroalgae, *Biogeosciences*, 10, 3615–3633, doi:10.5194/bg-10-3615-2013, 2013.

Liang, Q., Stolarski, R. S., Kawa, S. R., Nielsen, J. E., Douglass, A. R., Rodriguez, J. M., Blake, D. R., Atlas, E. L., and Ott, L. E.: Finding the missing stratospheric Br_y: a global modeling study of CHBr₃ and CH₂Br₂, *Atmos. Chem. Phys.*, 10, 2269–2286, doi:10.5194/acp-10-2269-2010, 2010.

Lin, S.-J.: A “vertically lagrangian” finite-volume dynamical core for global models, *Mon. Weather Rev.*, 132, 2293–2307, doi:10.1175/1520-0493(2004)132<2293:AVLFDC>2.0.CO;2, 2004.

**Bromine partitioning
in the TTL**

R. P. Fernandez et al.

Title Page

Abstract

Introduction

Conclusions

References

Tables

Figures



Back

Close

Full Screen / Esc

Printer-friendly Version

Interactive Discussion



- Liu, Y., Yvon-Lewis, S. a., Thornton, D. C. O., Butler, J. H., Bianchi, T. S., Campbell, L., Hu, L., and Smith, R. W.: Spatial and temporal distributions of bromoform and dibromomethane in the Atlantic Ocean and their relationship with photosynthetic biomass, *J. Geophys. Res.-Oceans*, 118, 1–16, doi:10.1002/jgrc.20299, 2013.
- 5 Marcy, T. P., Fahey, D. W., Gao, R. S., Popp, P. J., Richard, E. C., Thompson, T. L., Rosenlof, K. H., Ray, E. A., Salawitch, R. J., Atherton, C. S., Bergmann, D. J., Ridley, B. A., Weinheimer, A. J., Loewenstein, M., Weinstock, E. M., and Mahoney, M. J.: Quantifying stratospheric ozone in the upper troposphere with in situ measurements of HCl, *Science*, 304, 261–265, doi:10.1126/science.1093418, 2004.
- 10 Marsh, D. R., Mills, M. J., Kinnison, D. E., Lamarque, J.-F., Calvo, N., and Polvani, L. M.: Climate change from 1850 to 2005 simulated in CESM1(WACCM), *J. Climate*, 26, 7372–7391, doi:10.1175/JCLI-D-12-00558.1, 2013.
- McFiggans, G., Plane, J. M. C., Allan, B. J., Carpenter, L. J., Coe, H., and O'Dowd, C.: A modeling study of iodine chemistry in the marine boundary layer, *J. Geophys. Res.*, 105, 14371–14385, doi:10.1029/1999JD901187, 2000.
- 15 Meinshausen, M., Smith, S. J., Calvin, K., Daniel, J. S., Kainuma, M. L. T., Lamarque, J.-F., Matsumoto, K., Montzka, S. A., Raper, S. C. B., Riahi, K., Thomson, A., Velders, G. J. M., and Vuuren, D. P. P.: The RCP greenhouse gas concentrations and their extensions from 1765 to 2300, *Climatic Change*, 109, 213–241, doi:10.1007/s10584-011-0156-z, 2011.
- 20 Montzka, S. A., Reimann, S., Engel, A., Krüger, K., O'Doherty, S., and Sturges, W. T.: Ozone-depleting substances (ODSs) and related chemicals, in: *Scientific Assessment of Ozone Depletion: 2010*, chap. 1, Global Ozone Research and Monitoring Project-Report No. 52, Geneva, Switzerland, 1.1–1.108, 2011.
- Murphy, D. M., Fahey, D. W., Proffitt, M. H., Liu, S. C., Chan, K. R., Eubank, C. S., Kawa, S. R., and Kelly, K. K.: Reactive nitrogen and its correlation with ozone in the lower stratosphere and upper troposphere, *J. Geophys. Res.*, 98, 8751–8773, doi:10.1029/92JD00681, 1993.
- 25 Neale, R. B., Richter, J., Park, S., Lauritzen, P. H., Vavrus, S. J., Rasch, P. J., and Zhang, M.: The mean climate of the Community Atmosphere Model (CAM4) in forced SST and fully coupled experiments, *J. Climate*, 26, 5150–5168, doi:10.1175/JCLI-D-12-00236.1, 2013.
- 30 Neu, J. L. and Prather, M. J.: Toward a more physical representation of precipitation scavenging in global chemistry models: cloud overlap and ice physics and their impact on tropospheric ozone, *Atmos. Chem. Phys.*, 12, 3289–3310, doi:10.5194/acp-12-3289-2012, 2012.

**Bromine partitioning
in the TTL**

R. P. Fernandez et al.

Title Page

Abstract

Introduction

Conclusions

References

Tables

Figures



Back

Close

Full Screen / Esc

Printer-friendly Version

Interactive Discussion



- Ordóñez, C., Lamarque, J.-F., Tilmes, S., Kinnison, D. E., Atlas, E. L., Blake, D. R., Sousa Santos, G., Brasseur, G., and Saiz-Lopez, A.: Bromine and iodine chemistry in a global chemistry-climate model: description and evaluation of very short-lived oceanic sources, *Atmos. Chem. Phys.*, 12, 1423–1447, doi:10.5194/acp-12-1423-2012, 2012.
- 5 Parrella, J. P., Jacob, D. J., Liang, Q., Zhang, Y., Mickley, L. J., Miller, B., Evans, M. J., Yang, X., Pyle, J. A., Theys, N., and Van Roozendael, M.: Tropospheric bromine chemistry: implications for present and pre-industrial ozone and mercury, *Atmos. Chem. Phys.*, 12, 6723–6740, doi:10.5194/acp-12-6723-2012, 2012.
- 10 Pyle, J. A., Ashfold, M. J., Harris, N. R. P., Robinson, A. D., Warwick, N. J., Carver, G. D., Gostlow, B., O'Brien, L. M., Manning, A. J., Phang, S. M., Yong, S. E., Leong, K. P., Ung, E. H., and Ong, S.: Bromoform in the tropical boundary layer of the Maritime Continent during OP3, *Atmos. Chem. Phys.*, 11, 529–542, doi:10.5194/acp-11-529-2011, 2011.
- Quack, B. and Wallace, D. W. R.: Air–sea flux of bromoform: controls, rates, and implications, *Global Biogeochem. Cy.*, 17, 1023, doi:10.1029/2002GB001890, 2003.
- 15 Rayner, N. A.: Global analyses of sea surface temperature, sea ice, and night marine air temperature since the late nineteenth century, *J. Geophys. Res.*, 108, 4407, doi:10.1029/2002JD002670, 2003.
- Saiz-Lopez, A. and von Glasow, R.: Reactive halogen chemistry in the troposphere, *Chem. Soc. Rev.*, 41, 6448–6472, doi:10.1039/c2cs35208g, 2012.
- 20 Saiz-Lopez, A., Lamarque, J.-F., Kinnison, D. E., Tilmes, S., Ordóñez, C., Orlando, J. J., Conley, A. J., Plane, J. M. C., Mahajan, A. S., Sousa Santos, G., Atlas, E. L., Blake, D. R., Sander, S. P., Schauffler, S., Thompson, A. M., and Brasseur, G.: Estimating the climate significance of halogen-driven ozone loss in the tropical marine troposphere, *Atmos. Chem. Phys.*, 12, 3939–3949, doi:10.5194/acp-12-3939-2012, 2012.
- 25 Salawitch, R. J.: Atmospheric chemistry: biogenic bromine, *Nature*, 439, 275–277, doi:10.1038/439275a, 2006.
- Salawitch, R. J., Weisenstein, D. K., Kovalenko, L. J., Sioris, C. E., Wennberg, P. O., Chance, K., Ko, M. K. W., and McLinden, C. A.: Sensitivity of ozone to bromine in the lower stratosphere, *Geophys. Res. Lett.*, 32, L05811, doi:10.1029/2004GL021504, 2005.
- 30 Sander, R.: Compilation of Henry's Law Constants for Inorganic and Organic Species of Potential Importance in Environmental Chemistry (v3), available at: <http://www.henrys-law.org/> (last access 28 May 2014), 1999.

**Bromine partitioning
in the TTL**

R. P. Fernandez et al.

Title Page

Abstract

Introduction

Conclusions

References

Tables

Figures



Back

Close

Full Screen / Esc

Printer-friendly Version

Interactive Discussion



Sander, R. and Crutzen, P. J.: Model study indicating halogen activation and ozone destruction in polluted air masses transported to the sea, *J. Geophys. Res.*, 101, 9121–9138, doi:10.1029/95JD03793, 1996.

Sander, S. P., Friedl, R. R., Barker, J. R., Golden, D. M., Kurylo, M. J., Sciences, G. E., Wine, P. H., Abbatt, J. P. D., Burkholder, J. B., Kolb, C. E., Moortgat, G. K., Huie, R. E., and Orkin, V. L.: Chemical Kinetics and Photochemical Data for Use in Atmospheric Studies, Evaluation No. 17, JPL_NASA, 10-6(17), Jet Propulsion Laboratory, Pasadena, CA, 2011.

Sinnhuber, B.-M. and Folkins, I.: Estimating the contribution of bromoform to stratospheric bromine and its relation to dehydration in the tropical tropopause layer, *Atmos. Chem. Phys.*, 6, 4755–4761, doi:10.5194/acp-6-4755-2006, 2006.

Sinnhuber, B.-M., Sheode, N., Sinnhuber, M., Chipperfield, M. P., and Feng, W.: The contribution of anthropogenic bromine emissions to past stratospheric ozone trends: a modelling study, *Atmos. Chem. Phys.*, 9, 2863–2871, doi:10.5194/acp-9-2863-2009, 2009.

Sommariva, R. and von Glasow, R.: Multiphase halogen chemistry in the tropical Atlantic Ocean, *Environ. Sci. Technol.*, 46, 10429–10437, doi:10.1021/es300209f, 2012.

Thompson, A. M., Witte, J., Oltmans, S., Schmidlin, F., Logan, J., Fujiwara, M., Kirchhoff, V., Posny, F., Coetzee, G., Hoegger, B., Kawakami, S., Ogawa, T., Fortuin, J. P. F., and Kelder, H.: Southern Hemisphere Additional Ozonesondes (SHADOZ) 1998–2000 tropical ozone climatology 2. Tropospheric variability and the zonal wave-one, *J. Geophys. Res.*, 108, 8241, doi:10.1029/2002JD002241, 2003.

Tilmes, S., Kinnison, D. E., Garcia, R. R., Salawitch, R., Canty, T., Lee-Taylor, J., Madronich, S., and Chance, K.: Impact of very short-lived halogens on stratospheric ozone abundance and UV radiation in a geo-engineered atmosphere, *Atmos. Chem. Phys.*, 12, 10945–10955, doi:10.5194/acp-12-10945-2012, 2012.

Warwick, N. J., Pyle, J. A., Carver, G. D., Yang, X., Savage, N. H., O'Connor, F. M., and Cox, R. A.: Global modeling of biogenic bromocarbons, *J. Geophys. Res.*, 111, D24305, doi:10.1029/2006JD007264, 2006.

Wegner, T., Kinnison, D. E., Garcia, R. R., and Solomon, S.: Simulation of polar stratospheric clouds in the specified dynamics version of the whole atmosphere community climate model, *J. Geophys. Res.-Atmos.*, 118, 4991–5002, doi:10.1002/jgrd.50415, 2013.

Williams, J. E., Van Zadelhoff, G., and Scheele, M. P.: The Effect of Updating Scavenging and Conversion Rates on Cloud Droplets and Ice Particles in the Global Chemistry Trans-

port Model, KNMI Tech. Rep., Koninklijk Nederlands Meteorologisch Instituut, De Bilt, the Netherlands, TR-308, 45 pp., 2009.

Wisher, A., Oram, D. E., Laube, J. C., Mills, G. P., van Velthoven, P., Zahn, A., and Brenninkmeijer, C. A. M.: Very short-lived bromomethanes measured by the CARIBIC observatory over the North Atlantic, Africa and Southeast Asia during 2009–2013, *Atmos. Chem. Phys.*, 14, 3557–3570, doi:10.5194/acp-14-3557-2014, 2014.

Yang, X., Cox, R. A., Warwick, N. J., Pyle, J. A., Carver, G. D., O'Connor, F. M., and Savage, N. H.: Tropospheric bromine chemistry and its impacts on ozone: a model study, *J. Geophys. Res.*, 110, D23311, doi:10.1029/2005JD006244, 2005.

Ziska, F., Quack, B., Abrahamsson, K., Archer, S. D., Atlas, E., Bell, T., Butler, J. H., Carpenter, L. J., Jones, C. E., Harris, N. R. P., Hepach, H., Heumann, K. G., Hughes, C., Kuss, J., Krüger, K., Liss, P., Moore, R. M., Orlikowska, A., Raimund, S., Reeves, C. E., Reifenhäuser, W., Robinson, A. D., Schall, C., Tanhua, T., Tegtmeier, S., Turner, S., Wang, L., Wallace, D., Williams, J., Yamamoto, H., Yvon-Lewis, S., and Yokouchi, Y.: Global sea-to-air flux climatology for bromoform, dibromomethane and methyl iodide, *Atmos. Chem. Phys.*, 13, 8915–8934, doi:10.5194/acp-13-8915-2013, 2013.

ACPD

14, 17857–17905, 2014

Bromine partitioning in the TTL

R. P. Fernandez et al.

Title Page

Abstract

Introduction

Conclusions

References

Tables

Figures

◀

▶

◀

▶

Back

Close

Full Screen / Esc

Printer-friendly Version

Interactive Discussion



Bromine partitioning
in the TTL

R. P. Fernandez et al.

Table 1. Global annual oceanic flux, SG_{VSL} abundances and atmospheric lifetime of VSL bromocarbons.

Source Gas	Global Flux (Gg Br yr ⁻¹)	Lifetime ^a (days)	Surface vmr ^b (pptv of Br)	Lower TTL ^b (~ 12 km) (CAM-Chem)	Lower TTL (~ 12 km) (WMO-2010)	Upper TTL (~ 17 km) (CAM-Chem)	Upper TTL ^b (~ 17 km) (WMO-2010)
CHBr ₃	505.6	17	5.5	1.89	(0.9–3.3)	0.20	(0.03–0.87)
CH ₂ Br ₂	61.9	130	2.2	1.82	(1.54–2.30)	1.5	(0.86–1.66)
CH ₂ BrCl	6.2	145	0.3	0.21	(0.13–0.16)	0.19	(0.1–0.12)
CHBr ₂ Cl	15.1	56	0.4	0.24	(0.12–0.30)	0.06	(0.02–0.22)
CHBrCl ₂	11.0	46	0.2	0.14	(0.18–0.22)	0.05	(0.11–0.14)
CH ₂ IBr	31.6	0.1	0.01	~ 0	Not reported	~ 0	Not reported
Total	631.4	–	8.5	4.30	(2.86–6.5)	2.0	(1.1–3.2)

Adapted from Table 3 in Ordoñez et al. (2012) and Tables 1–7 from WMO-2010 (Montzka et al., 2011). The vmr for each species have been multiplied by their respective atomicity in order to represent the contribution to Br_y.

^a Lifetimes for each species have been computed considering tropospheric loss by photolysis and reaction with OH.

^b Values are in pptv of Br, and have been averaged for the tropical latitudinal band (20° N–20° S).

Title Page

Abstract

Introduction

Conclusions

References

Tables

Figures

◀

▶

◀

▶

Back

Close

Full Screen / Esc

Printer-friendly Version

Interactive Discussion



Bromine partitioning
in the TTL

R. P. Fernandez et al.

Title Page

Abstract

Introduction

Conclusions

References

Tables

Figures

◀

▶

◀

▶

Back

Close

Full Screen / Esc

Printer-friendly Version

Interactive Discussion

**Table 2.** Description of inputs for various box-model simulations.

Simulation	Particle Type	Surface Area (SA) ($\text{cm}^2 \text{cm}^{-3}$)	$\gamma_{\text{HOBr}+\text{HBr}}$	Cl_y (pptv)
<i>Run_0</i>	Sulfate	2.9×10^{-8}	0.0	0.0
<i>Run_1a</i>	Sulfate	2.9×10^{-8}	0.25	0.0
<i>Run_1b</i>	Ice	1.8×10^{-5}	0.1	0.0
<i>Run_2a</i>	Sulfate	2.9×10^{-8}	0.25	50.0
<i>Run_2b</i>	Ice	1.8×10^{-5}	0.1	50.0

Bromine partitioning
in the TTL

R. P. Fernandez et al.

Title Page

Abstract

Introduction

Conclusions

References

Tables

Figures

◀

▶

◀

▶

Back

Close

Full Screen / Esc

Printer-friendly Version

Interactive Discussion

**Table 3.** Description of the CAM-Chem setup used for different global sensitivity simulations.

Simulation name	Description
<i>cam_Full_Br</i>	Considers all SG_{VSL} and Long-Lived (LL) sources
<i>cam_NoVSL</i>	Considers only LL sources and no SG_{VSL}
<i>cam_CHBr3</i>	Considers only $CHBr_3$ and LL sources
<i>cam_CH2Br2</i>	Considers only CH_2Br_2 and LL sources
<i>cam_MinorVSL</i>	Considers CH_2BrCl , $CHBr_2Cl$, $CHBrCl_2$, CH_2IBr and LL sources
<i>cam_NoSSLT</i>	Same sources as <i>cam_Full_Br</i> . Recycling reactions over sea-salt aerosols had been turned OFF*

* Heterogeneous reactions HSS0-HSS5 of Table S1 in the Supplement have not been considered.

Bromine partitioning
in the TTL

R. P. Fernandez et al.

Table 4. Partitioning of source gas (SG_{VSL}) and product gas (PG_{VSL}) species within the TTL for different CAM-Chem simulations.

Region (Period)	Tropical Average (Annual) ^b				Western Pacific (Feb) ^c				Vigorous Event (3 days) ^d			
	Upper TTL (17 km)				Upper TTL (17 km)				Upper TTL (17 km)			
Sensitivity	PG _{VSL}	SG _{VSL}	ΣBr	R	PG _{VSL}	SG _{VSL}	ΣBr	R	PG _{VSL}	SG _{VSL}	ΣBr	R
<i>cam_Full_Br</i>	3.0	2.0	5.0	1.5	3.9	3.9	7.8	1.0	3.0	4.6	7.6	0.6
<i>cam_NoVSL</i> ^a	0.6	15.6	16.2	0.04	0.4	16.3	16.7	0.02	0.2	16.3	16.5	0.01
<i>cam_CHBr3</i>	2.5	0.2	2.7	9.5	3.1	1.3	4.4	2.1	2.5	2.0	4.5	1.2
<i>cam_CH2Br2</i>	1.1	1.5	2.6	0.3	0.7	1.9	2.6	0.2	0.5	1.9	2.4	0.2
<i>cam_MinorVSL</i>	1.1	0.3	1.4	1.7	2.1	0.6	2.7	2.8	1.8	0.7	2.5	2.3
<i>cam_NoSSLT</i>	2.9	2.0	4.9	1.4	1.8	3.8	5.6	0.5	0.8	4.6	5.4	0.2
	Lower TTL (12 km)				Lower TTL (12 km)				Lower TTL (12 km)			
	PG _{VSL}	SG _{VSL}	ΣBr	R	PG _{VSL}	SG _{VSL}	ΣBr	R	PG _{VSL}	SG _{VSL}	ΣBr	R
<i>cam_Full_Br</i>	1.0	4.3	5.3	0.2	2.5	5.1	7.6	0.5	3.6	5.7	9.3	0.6
<i>cam_NoVSL</i> ^a	0.05	16.3	16.4	0.003	0.4	16.4	16.8	0.02	0.3	16.4	16.7	0.01
<i>cam_CHBr3</i>	0.9	1.9	2.8	0.5	2.4	2.4	4.8	0.8	3.7	3.0	6.7	1.1
<i>cam_CH2Br2</i>	0.2	1.8	2.0	0.1	0.6	2.0	2.6	0.1	2.9	2.0	4.9	1.3
<i>cam_MinorVSL</i>	0.2	0.6	0.8	0.3	1.4	0.7	2.1	1.4	3.0	0.7	3.7	3.9
<i>cam_NoSSLT</i>	0.9	4.3	5.1	0.2	0.9	5.0	5.9	0.2	0.5	5.7	6.2	0.08

All values with exception of the *R* quotient are reported in parts per trillion by volume (pptv).

ΣBr = SG_{VSL} + PG_{VSL} is the total bromine loading from VSL sources.

R = PG_{VSL}/SG_{VSL} for the *cam_Full_Br*, *cam_NoVSL* and *cam_NoSSLT* runs whereas *R* = (PG_{VSL} - PG_{cam_NoVSL})/SG_{VSL} for the *cam_CHBr3*, *cam_CH2Br2*, and *cam_MinorVSL* runs.

PG_{cam_NoVSL} is subtracted from PG_{VSL} to account for stratospheric injection of product gases resulting from tropospheric degradation of CH₃Br, which was present in the *cam_CHBr3*, *cam_CH2Br2*, and *cam_MinorVSL* simulations.

^a For *cam_NoVSL* sensitivity, PG_{VSL} and SG_{VSL} represent the inorganic and organic contributions from Long-Lived sources.

^b 24 h annual tropical average has been computed for the (20° N–20° S) latitudinal band.

^c 24 h monthly averages for February within the WP region outlined in black in Fig. 5.

^d Noontime 3 days average for a vigorous event within the WP region.

Title Page

Abstract

Introduction

Conclusions

References

Tables

Figures

◀

▶

◀

▶

Back

Close

Full Screen / Esc

Printer-friendly Version

Interactive Discussion



Bromine partitioning
in the TTL

R. P. Fernandez et al.

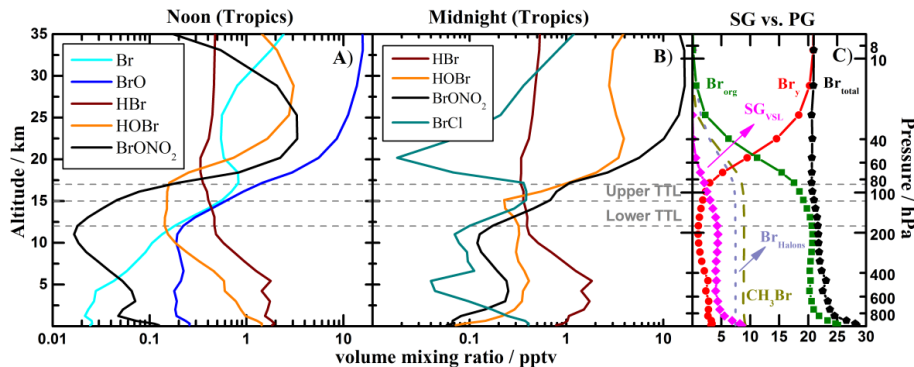


Figure 1. Annual vertical profile abundances of organic and inorganic bromine species within the tropics (20°N–20°S): **(A)** main Br_y species at noon; **(B)** main Br_y species at midnight; and **(C)** 24 h average contribution of organic and inorganic species to total bromine. The horizontal dotted lines represent the approximate location of the TTL.

Bromine partitioning
in the TTL

R. P. Fernandez et al.

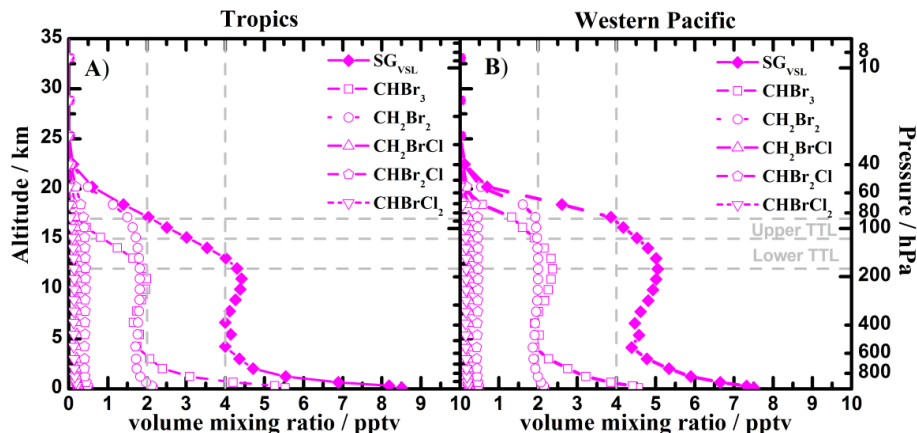


Figure 2. Vertical profile abundances of the five VSL bromocarbons considered in CAM-Chem for the tropical annual average (A) and the Western Pacific region (B). All halocarbon abundances are multiplied by their respective atomicity in order to represent their contribution to Br_y after photolysis or reaction with OH. The total organic SG_{VSL} contribution is also shown by the filled diamonds.

Title Page

Abstract

Introduction

Conclusions

References

Tables

Figures

◀

▶

◀

▶

Back

Close

Full Screen / Esc

Printer-friendly Version

Interactive Discussion



Bromine partitioning
in the TTL

R. P. Fernandez et al.

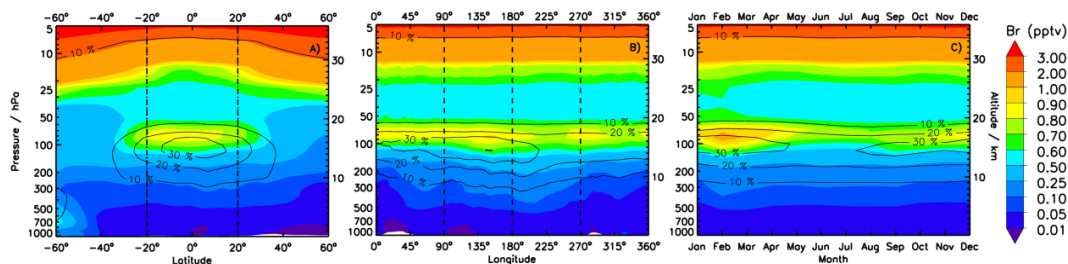


Figure 3. The “tropical ring of atomic bromine”: **(A)** annual zonal average; **(B)** annual meridional average abundance of atomic Br within the tropics (20°N – 20°S); and **(C)** seasonal evolution of the zonally-averaged atomic Br ring within the tropics. The color scale represents noontime volume mixing ratios (pptv) while black contour lines show the percentage contribution of atomic Br to Br_y .

Title Page

Abstract

Introduction

Conclusions

References

Tables

Figures



Back

Close

Full Screen / Esc

Printer-friendly Version

Interactive Discussion



Bromine partitioning
in the TTL

R. P. Fernandez et al.

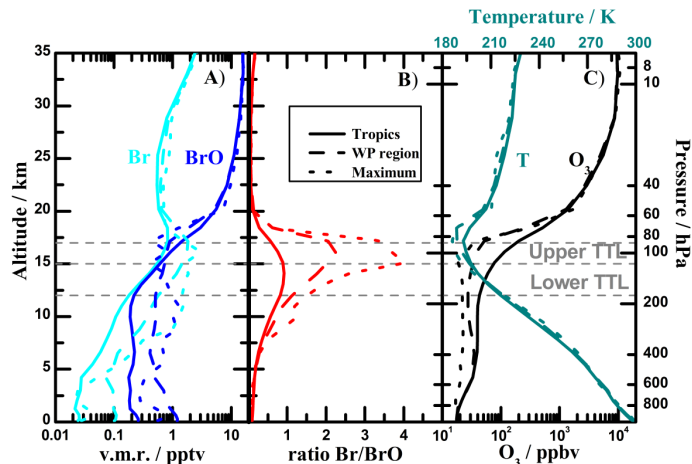


Figure 4. Vertical noontime profiles of **(A)** Br and BrO vmr, **(B)** the Br/BrO ratio, and **(C)** T and O_3 in the tropics. Vertical profiles have been averaged over different regions and time periods: (solid) annual tropical averages (20°N – 20°S); (dashed) WP region during February; (dotted) at the midpoint of a strong convective cell within the WP during a 3 day period in February.

Title Page

Abstract

Introduction

Conclusions

References

Tables

Figures



Back

Close

Full Screen / Esc

Printer-friendly Version

Interactive Discussion



Bromine partitioning
in the TTL

R. P. Fernandez et al.

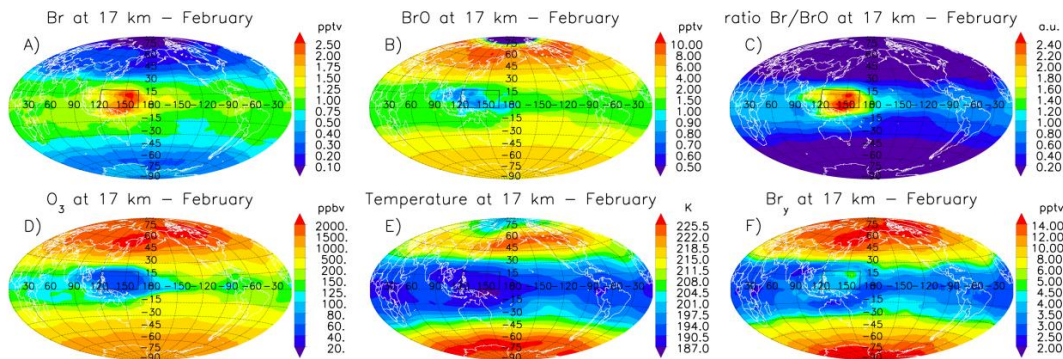


Figure 5. Average noontime geographical distribution of atmospheric bromine, ozone and temperature at 17 km during February: **(A)** atomic Br; **(B)** BrO; **(C)** Br/BrO ratio; **(D)** ozone; **(E)** temperature; and **(F)** Br₂. The location of the WP region, also considered to compute the vertical profiles of Figs. 4 and 11 is outlined in black.

Title Page

Abstract

Introduction

Conclusions

References

Tables

Figures



Back

Close

Full Screen / Esc

Printer-friendly Version

Interactive Discussion



Bromine partitioning
in the TTL

R. P. Fernandez et al.

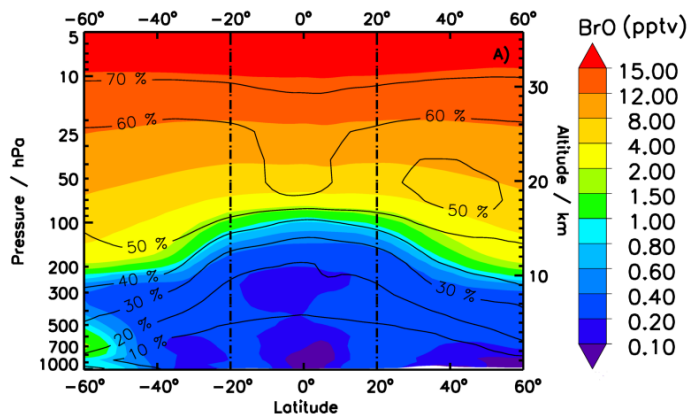


Figure 6. Annual daytime zonal average BrO distributions between 60° N–60° S. The color scale represents absolute values (pptv), while black contour lines show the percentage contribution of BrO to Br_y.

[Title Page](#)[Abstract](#)[Introduction](#)[Conclusions](#)[References](#)[Tables](#)[Figures](#)[◀](#)[▶](#)[◀](#)[▶](#)[Back](#)[Close](#)[Full Screen / Esc](#)[Printer-friendly Version](#)[Interactive Discussion](#)

Bromine partitioning
in the TTL

R. P. Fernandez et al.

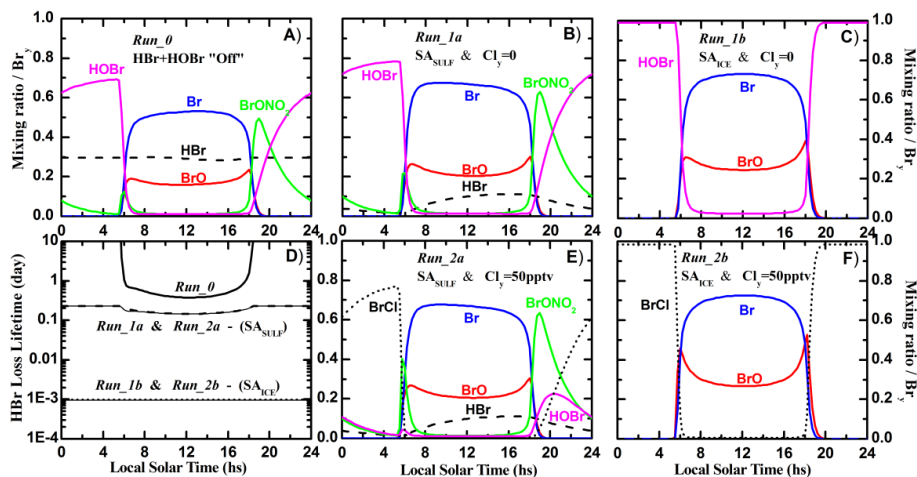


Figure 7. Calculated abundance of inorganic bromine species as a function of local solar time for different sensitivity simulations: **(A)** *Run_0* (SA_{SULF} ; $\gamma_{HOBr+HBr} = 0$; $Cl_y = 0$); **(B)** *Run_1a* (SA_{SULF} ; $\gamma_{HOBr+HBr} = 0.25$; $Cl_y = 0$); **(C)** *Run_1b* (SA_{SULF} ; $\gamma_{HOBr+HBr} = 0.25$; $Cl_y = 50$ pptv); **(D)** photochemical lifetime of HBr for all 5 sensitivity simulations; **(E)** *Run_2a* (SA_{ICE} ; $\gamma_{HOBr+HBr} = 0.1$; $Cl_y = 0$); **(F)** *Run_2b* (SA_{ICE} ; $\gamma_{HOBr+HBr} = 0.1$; $Cl_y = 50$ pptv). Box model simulations were performed for Lat = 10° N and Solar Decl = 20° , with the following atmospheric conditions: $p = 130$ hPa, $T = 200$ K, $H_2O = 12.5$ ppmv, $CH_4 = 1.77$ ppmv, $CO = 60$ ppbv, $Br_y = 4$ pptv, $NO_y = 400$ pptv and $O_3 = 25$ ppbv.

Title Page

Abstract

Introduction

Conclusions

References

Tables

Figures



Back

Close

Full Screen / Esc

Printer-friendly Version

Interactive Discussion



Bromine partitioning
in the TTL

R. P. Fernandez et al.

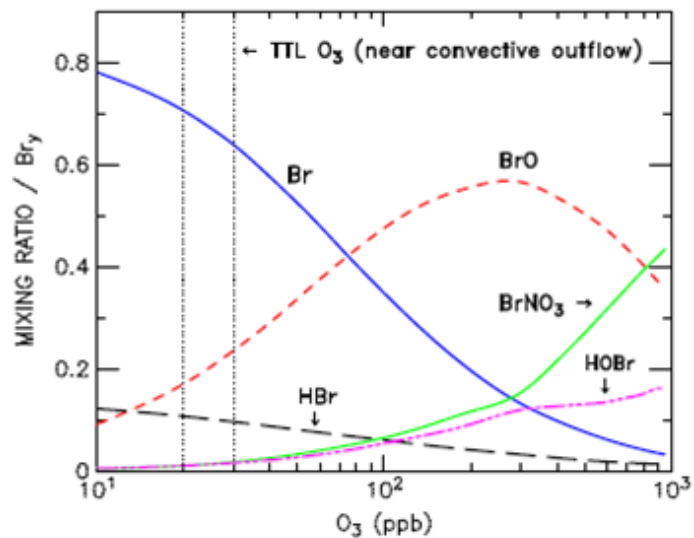


Figure 8. Box-model partitioning of Br_y species as a function of ozone mixing ratio. The abundances (normalized to total Br_y) are from diurnal photochemical steady state conditions at local noon. Inputs for aerosol surface area, inorganic chlorine, and $\gamma_{\text{HOBr}+\text{HBr}}$ are for *Run_1a*.

Title Page

Abstract

Introduction

Conclusions

References

Tables

Figures

◀

▶

◀

▶

Back

Close

Full Screen / Esc

Printer-friendly Version

Interactive Discussion



Bromine partitioning
in the TTL

R. P. Fernandez et al.

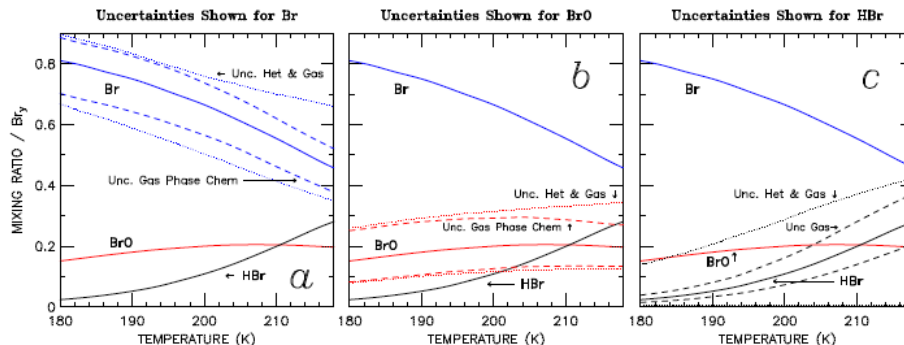


Figure 9. Temperature dependence of the calculated abundance of atomic Br, BrO and HBr at local noon. The baseline simulation (solid line) assumes conditions for SA, Cl_y , and $\gamma_{HOBr+HBr}$ from *Run_1a*: **(A)** atomic Br uncertainties considering only gas phase processes (dashed lines) and combined uncertainty considering both heterogeneous and gas phase processes (dotted lines). Uncertainties for BrO and HBr are shown in **(B)** and **(C)**, respectively.

Title Page

Abstract

Introduction

Conclusions

References

Tables

Figures

◀

▶

◀

▶

Back

Close

Full Screen / Esc

Printer-friendly Version

Interactive Discussion



Bromine partitioning
in the TTL

R. P. Fernandez et al.

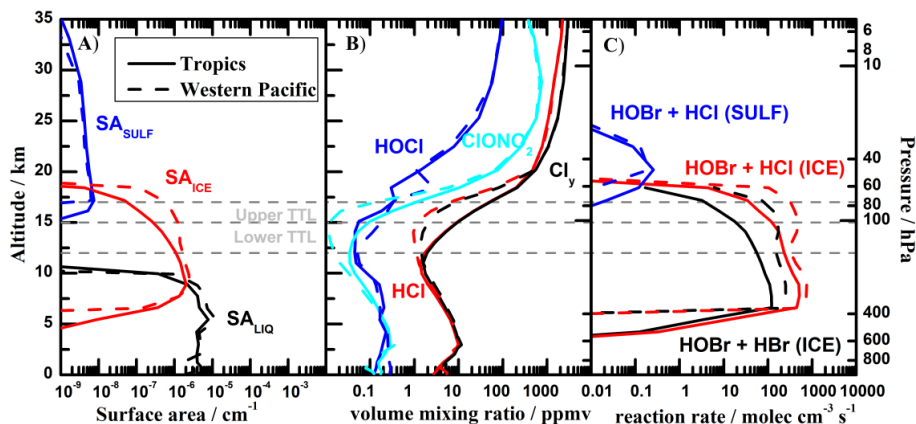


Figure 10. Vertical variation of CAM-Chem atmospheric constituents affecting the rate of heterogeneous reactions within the tropics (solid lines) and WP region (dotted lines): **(A)** surface area for ice particles (SA_{ICE}), liquid droplets (SA_{LIQ}) and sulphate aerosols (SA_{SULF}); **(B)** average vertical profiles of HCl, HOCl, $ClONO_2$ and total inorganic chlorine (Cl_y); **(C)** heterogeneous reaction rates over different types of surfaces.

Title Page

Abstract

Introduction

Conclusions

References

Tables

Figures

◀

▶

◀

▶

Back

Close

Full Screen / Esc

Printer-friendly Version

Interactive Discussion



Bromine partitioning
in the TTL

R. P. Fernandez et al.

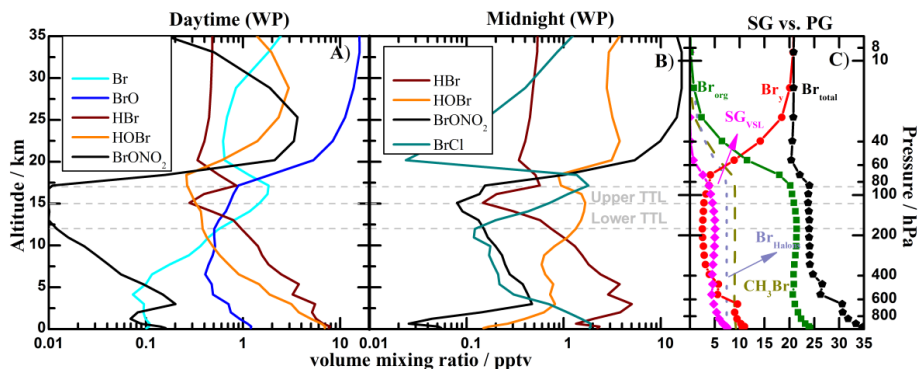


Figure 11. Vertical profile abundances of organic and inorganic bromine species within the WP region during February: **(A)** main Br_y species at noon; **(B)** main Br_y species at midnight; and **(C)** 24 h average contribution of organic and inorganic species to total bromine.

Title Page

Abstract

Introduction

Conclusions

References

Tables

Figures

◀

▶

◀

▶

Back

Close

Full Screen / Esc

Printer-friendly Version

Interactive Discussion

